nature communications

Article

https://doi.org/10.1038/s41467-024-52113-y

HIF-2α-dependent induction of miR-29a restrains T_H1 activity during T cell dependent colitis

Received: 19 January 2023

Accepted: 22 August 2024

Published online: 14 September 2024

Check for updates

Agnieszka K. Czopik[1,14] ✉, Eóin N. McNamee[2,3,14], Victoria Vaughn[1], Xiangsheng Huang[1], In Hyuk Bang[1], Trent Clark[1], Yanyu Wang[1], Wei Ruan[1], Tom Nguyen[2,3], Joanne C. Masterson[2,4,5], Eunyoung Tak[3,6], Sandra Frank[7,8], Colm B. Collins[2,5], Howard Li[9], Cristian Rodriguez-Aguayo[10], Gabriel Lopez-Berestein[10], Mark E. Gerich[2,11], Glenn T. Furuta[2,4,5], Xiaoyi Yuan[1], Anil K. Sood[10,12], Edwin F. de Zoeten[2,5] ✉ & Holger K. Eltzschig[1,13]

Metabolic imbalance leading to inflammatory hypoxia and stabilization of hypoxia-inducible transcription factors (HIFs) is a hallmark of inflammatory bowel diseases. We hypothesize that HIF could be stabilized in $CD4^+$ T cells during intestinal inflammation and alter the functional responses of T cells via regulation of microRNAs. Our assays reveal markedly increased T cell-intrinsic hypoxia and stabilization of HIF protein during experimental colitis. microRNA screen in primary $CD4^+$ T cells points us towards miR-29a and our subsequent studies identify a selective role for HIF-2α in CD4-cell-intrinsic induction of miR-29a during hypoxia. Mice with T cell-intrinsic *HIF-2α* deletion display elevated T-bet (target of miR-29a) levels and exacerbated intestinal inflammation. Mice with *miR-29a* deficiency in T cells show enhanced intestinal inflammation. T cell-intrinsic overexpression of *HIF-2α* or delivery of miR-29a mimetic dampen T_H1-driven colitis. In this work, we show a previously unrecognized function for hypoxia-dependent induction of miR-29a in attenuating T_H1-mediated inflammation.

The intestines contain the most significant number of immune cells of any tissue in the body and are a site for considerable immunologic activity. With the central role of oxygen metabolism and the physiological characteristics of this organ, intestinal homeostasis is highly dependent on adaptive pathways activated by hypoxia-dependent transcriptional programs. During inflammatory bowel diseases (IBD), a marked increase in intestinal inflammatory hypoxia and stabilization of the HIF (*hypoxia-inducible factor)* transcription factors occurs due to increased metabolic demand and a paucity of available oxygen[1–7]. The increased localized hypoxia during intestinal inflammation has been attributed partially to transmigrating neutrophils, which utilize respiratory bursts to rapidly and locally deplete oxygen during inflammation[8]. In the inflamed mucosa, HIF signaling elicits protective immune responses, increases barrier genes, and maintains the intestine's regenerative and proliferative capacity, leading to the resolution of inflammation[9–11].

$CD4^+$ helper T cells play a critical role in coordinating immune responses to pathogens. At the same time, their unrestrained activation drives chronic pathologies, which contribute centrally to the pathogenesis of inflammatory bowel diseases. Evidence for the $CD4^+$ T_H1 cell involvement in IBD inflammation comes from the prominent transmural infiltration associated with $IFN\gamma^+$ granulomata[12], while the T_H1 effector cytokines and the cardinal T_H1 transcription factor T-bet are significantly increased in active Crohn's disease lesions[13–15]. T-bet regulates differentiation cues of T_H1 T cells by directly driving T_H1 responses or by repressing T_H17 activation in T-bet-deficient mice within experimental models of colitis[15,16]. Production of IFNγ by the progeny of T_H17 cells is required for disease development in a transfer

A full list of affiliations appears at the end of the paper. ✉e-mail: Agnieszka.K.Czopik@uth.tmc.edu; Edwin.DeZoeten@childrenscolorado.org

model of colitis, and T-bet is indispensable for the induction of colitis, underscoring the central role for this transcription factor and for IFNγ signaling in colitic T cells[15]. While numerous reports explored the role of HIF factors in the development and intestinal function of T_H9, T_H17 and T_{reg} cells[3,17–20], our understanding of how hypoxic signaling affects T_H1 T cell function in intestinal inflammation remains limited.

Functional consequences of hypoxia can lead the induction of HIF target genes promoting cell survival under hypoxic conditions (such as erythropoietin). However, in many instances, HIF stabilization is associated with the repression of target genes[21], most commonly via the induction of hypoxia-inducible micro RNAs (miRNAs)[22,23]. miRNAs which are short, noncoding RNAs exerting post-transcriptional regulation of gene expression by targeting 3′UTR in a sequence-specific manner[24] have been shown as HIF targets and were implicated in attenuating inflammation[25–27]. Additionally, miRNAs play specialized suppressive roles during helper T cell development[28–30]. A genetic deficiency in the enzymes which process miRNA transcripts into their mature form leads to deficits in $CD4^+$ T cell functions including a bias towards IFNγ production[31]. Specifically, miR-29a directly regulates IFNγ expression and mice with miR-29a deficiency show increased resistance to intracellular bacterial infection but higher susceptibility to IFNγ-driven autoimmune disorders[32,33].

Here, we report the functional consequences of hypoxia within the inflamed intestine on the miRNA expression in helper T cells. We develop assays to measure T cell-specific hypoxia and HIF stabilization in vivo and find that colitogenic $CD4^+$ T cells undergo a marked increase in cellular hypoxia and stabilize HIF during active colitis. Our studies indicate that this hypoxic stimulation represses T-bet expression and IFNγ production from T_H1 T cells in a HIF-2α-dependent manner. Therefore, in this work, we uncover a central role of hypoxia-signaling in the negative feedback regulation of T_H1 T cell expansion during intestinal inflammation via the transcriptional induction of immunologic active miRNAs.

Results

Colitogenic $CD4^+$ T cells become hypoxic and stabilize HIF

Tissue hypoxia is a hallmark of colitis[1,8], and previous studies have shown a protective role of HIFs in attenuating intestinal inflammation[34]. However, the knowledge about the role of the hypoxic microenvironment on the function of T helper cells is limited. Therefore, we pursued studies to visualize and quantify T cell-intrinsic hypoxia and concomitant HIF stabilization in murine models of intestinal inflammation in vivo. To assess T cell hypoxia across varying activation states, we administered 2-nitroimidazole (EF5) intravenously into mice with naïve T cell transfer-induced colitis, and followed by anti-EF5 labeling (EF5-Cy5). Resulting hypoxic adducts in T cells at fulminant disease were then analyzed by flow cytometry. We observed that effector-memory $CD4^+$ T cells (T_{EM}) in inflamed colons accumulate significant $EF5^+$ staining indicating decreased oxygen tension (hypoxia) in these cells (Fig. 1a). Similar $EF5^+$ staining pattern is evident in the longer-lasting effector-memory T cells (Fig. 1b). Increased staining intensities were observed in the intestinal compared to mesenteric lymph node or spleen T cells, in line with the ranked physiologic hypoxic gradients of these organs during intestinal inflammation[35].

Next, we designed a system to visualize the activation of T cell-intrinsic HIF stabilization within the inflamed colon utilizing adoptive transfer of naïve $CD4^+$ T cells ($CD4^+CD45RB^{high}$) from HIF-reporter mice ["B6ΔODD-luciferase mice"[36]] into host mice that do not express luciferase (Supplementary Fig. 1a). These mice were fully backcrossed onto C57BL/6J/6J background to allow for a transfer into a matching *Rag1*-deficient strain. At fulminant disease (7 weeks post-transfer, Supplementary Fig. 1b) luciferase activity derived solely from the hypoxic T cells was measured by whole-tissue imaging. While transferring $CD4^+CD45RB^{low}$ T cells resulted in a normal colon appearance and background levels of luciferase (Fig. 1c), the $CD4^+CD45RB^{high}$ T cell recipients exhibited severe colitis, documented by histological analysis which correlated with a marked increase in T cell-intrinsic HIF stabilization (Fig. 1d), and confirmed by measurements of the luciferase radiance signal intensity (Fig. 1e), with the colon inflammatory scores matching the luciferase and histological data (Fig. 1f). In comparison, the small intestines from the same colitic animals show similar background levels of luciferase activity (Supplementary Fig. 1c and Supplementary Fig. 1d). Taken together, the present studies demonstrate a $CD4^+$ T cell-intrinsic increase in hypoxia with a concomitant stabilization of HIF during active colitis in mice.

miR-29a is a hypoxia target in $CD4^+$ T cells

Based on our studies showing that $CD4^+$ T cells experience intrinsic hypoxia and concomitant HIF stabilization in colitis, we next pursued the transcriptional consequences of HIFs stabilization. While HIF is known to induce specific target genes (such as erythropoietin), in many instances HIF stabilization is associated with the repression of target genes[21], most commonly via the induction of hypoxia-inducible miRNAs[22,23]. Therefore, we examined T cell intrinsic transcriptional responses to ambient hypoxia on miRNA expression. For this purpose, we subjected $CD4^+$cells to brief activation (8 h) in normal oxygen conditions or in hypoxia (1% oxygen) and performed a limited T cell-focused miRNA expression array (Supplementary Data 1). This screen identified miR-29a as the leading miRNA candidate upon ambient hypoxia exposure of purified $CD4^+$ T cells (Fig. 2a). Mature miR-29s are highly conserved in human, mouse, and rat and share identical sequences at the seed region that plays a key role in determining their targets[37]. In addition, we also observed increased miR-29a expression in colonic pinch biopsies from inflammatory bowel disease (IBD) patients suffering from Crohn's disease (CD) or Ulcerative Colitis, which correlated with disease activity (Fig. 2b). Fractionation of colon from a healthy mouse demonstrates that miR-29a expression localizes largely to the lamina propria lymphocytes (LP), with comparatively lower level of expression in the intestinal epithelial cells (IEC) (Fig. 2c).

Next, we differentiated mouse $CD4^+$ T helper lineages (T_H0, T_H1, T_H2, T_H17, T_{reg}) and identified a significant upregulation of miR-29a following 8 h of ambient hypoxia exposure (1% O_2). This induction was highest in the T_H0 and T_H1 subsets (Fig. 2d). The hypoxia-driven increase in miR-29a was mirrored in whole primary human $CD4^+$ and differentiated T_H0 and T_H1 $CD4^+$ T cells cultured from peripheral blood mononuclear cells of healthy donors and subjected to similar activating regimen (Fig. 2e). Collectively, these studies identify that miR-29a is a T cell-expressed miRNA which shows increased expression during exposure to hypoxia, particularly in T_H1 T cells and potentially in other T cell subsets.

Induction of miR-29a in $CD4^+$ T cells is mediated by HIF-2α

Hif-1α and *Hif-2α* are closely related isoforms but genetic inactivation studies of each isoform in mice demonstrate substantially different phenotypes, suggesting that HIF-1α or HIF-2α control distinct transcriptional targets[38]. Therefore, we applied genetic studies to address the relative contributions of HIF-1α or HIF-2α to miR-29a induction during hypoxia. For this purpose, primary mouse $CD4^+$ T cells from mice with T cell-intrinsic HIF isoform deletions (*Hif-1α*$^{loxP/loxP}$ *Lck Cre*$^+$ or *Hif-2α*$^{loxP/loxP}$ *Lck Cre*$^+$ mice[18,39,40] were activated in vitro. Following 8 h of ambient hypoxia exposure (1% oxygen), miR-29a was significantly induced in T cells from control mice (*Lck Cre*$^+$) compared to *Hif-1α*-deficient T cells. In contrast, miR-29a induction was completely abolished in *Hif-2α*-deficient $CD4^+$ T cells (Fig. 3a). Conversely, $CD4^+$ T cells from mice with T cell-intrinsic HIF-2α stabilization [(*LSL-HIF2dPA Lck Cre*$^+$)[41]] displayed a significant induction of miR-29a under normoxia (Fig. 3b). Lastly, to assess if miR-29a induction can be achieved pharmacologically using a HIF-activator, we treated primary $CD4^+$ T cells from mice and humans with the cell permeable prolyl-hydroxylase inhibitor, dimethyloxaloylglycine (DMOG)[42]. Consistent with the above

https://doi.org/10.1038/s41467-024-52113-y

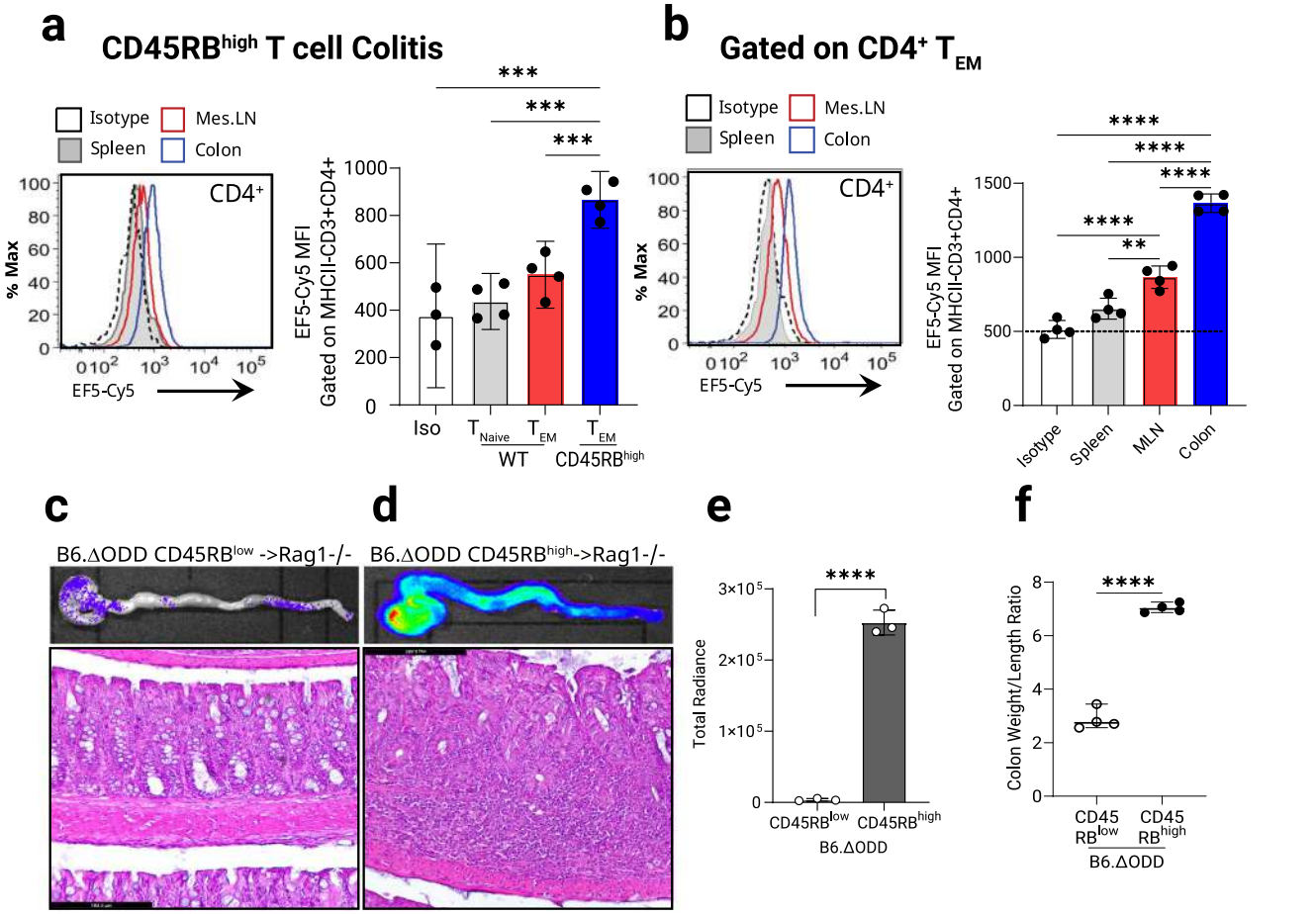

Fig. 1 | Stabilization of Hypoxia Inducible Factor in colitogenic CD4+ T cells during experimental colitis. Chronic T cell-mediated colitis was induced in B6.B6.RAG1−/− mice by intraperitoneal injection (0.5 × 106) of naïve CD4+ CD45RBhigh or CD45RBlow T cells. Identification of 2-nitroimidazole EF5 hypoxic adducts in B6.B6.RAG1−/− mice injected with C57BL/6J/6JT cells. 6 weeks post-treatment spleens, lymph nodes and collagenase-digested colon tissues were assessed. **a** Flow cytometric sub-analysis of cellular profile within Cy5-labeled EF5 (nitroimidazole; injected IP-3h) naïve and effector memory CD4+ T cells from the spleen, mesenteric lymph nodes and the colons, ($n = 3–4$, one-way ANOVA). **b** Effector memory CD4+ T cells from the spleen, mesenteric lymph node (MLN) and collagenase digested colons (gated on CD44 + CD62L−) and labeled with EF5-Cy5. Identification of stabilized HIF in dissected colons by IVIS imaging from mice adoptively transferred with 0.5 × 106 B6.ΔODD.luc CD4+ T cells. Prior to euthanizing, mice were injected with Luciferase substrate for 10 min. Freshly dissected colons were flushed and imaged using IVIS. Representative IVIS photograph and corresponding colon micrograph sections were stained with H&E, $n = 4$. **c** Healthy colons from CD45RBlow transferred mice, with low luciferase activity in the upper panel. Colon histological sections (lower panel, Scale bar: 184.4 mm). **d** High luciferase activity in whole colon (upper panel) and histology micrograph with lymphocyte infiltrates in CD45RBhigh transferred mice at 6-week post transfer (lower panel, Scale bar: 184.4 mm). **e** Image radiance was quantified using IVIS and expressed as photons/sec/cm2/sr. ($n = 3$, two-tailed T test). **f** Colon inflammation score (weight/length) in adoptively transferred animals from (**c**) and (**d**) ($n = 4$, two-tailed T test). Male and female mice used in (**a**) and (**b**), male recipients and male and female donors used in (**c**)–(**f**). Radiance of IVIS image was quantified and expressed as photons/sec/cm2/sr. Data expressed as Mean ±S.E.M., $^*p < 0.05$, $^{**}p < 0.01$, $^{***}p < 0.001$, $^{****}p < 0.0001$ vs. indicated.

studies in genetic models, DMOG treatment significantly induced miR-29a to levels comparable with the induction observed during hypoxia exposure (mouse cells Fig. 3c and human cells Fig. 3d). Furthermore, the levels of miR-29a in colonic biopsies of middle colon failed to increase in mice with *Hif-2α*-deficient CD4+ T cells compared to controls in a chronic DSS colitis model (Fig. 3e), although this increase may not be solely due to the T cell derived miR-29a.

Previously published analyses have confirmed that *miR-29b-1* and *miR-29a* are transcribed together as a polycistronic primary transcript with mature miR-29a localizing to the cytoplasm while miR-29b-1 predominantly localizes to the nucleus[37,43]. Analysis of the nucleotide sequence within the *miR-29b1-a* proximal promoter identifies 7 potential Hypoxia Responsive Elements (HRE)[44] and the 3 most proximal to the transcriptional start site are indicated on the diagram (Fig. 3f). We employed chromatin immunoprecipitation (ChIP) assay to address binding of HIF-2α to 3 individual proximal HREs that most closely conformed to the previously established criteria for functional HREs within 1 kb upstream of the transcriptional start site[44]. These studies demonstrate modest binding of HIF-2α to HRE#1 (Fig. 3g, first panel) but not to HRE#2 and HRE#3 (Fig. 3g, panels 2 and 3) during ambient hypoxia exposure of CD4+ T cells (4 more distal HREs were not tested in this assay). Together these studies point to a role for HIF-2α in the induction of miR-29a in CD4+ T cells during ambient hypoxia exposure.

miR-29a target T-bet is repressed in T_H1 T cells in hypoxia

Having identified a T cell-intrinsic role of HIF-2α in the induction of miR-29a, we next pursued studies to identify specific miR-29a target genes as a functional consequence of the increased expression of this microRNA. Among previously characterized miR-29a target genes, the T_H1 transcription factor *T-bet* (*Tbx21*) was shown to be a bona fide target[45] and T cell-intrinsic overexpression of miR-29a negatively regulated T-bet and a closely related transcription factor, Eomes[31]. Naive T cells activated under hypoxic conditions (1% oxygen) for 8 h rapidly increased expression of miR-29a compared to similarly

https://doi.org/10.1038/s41467-024-52113-y

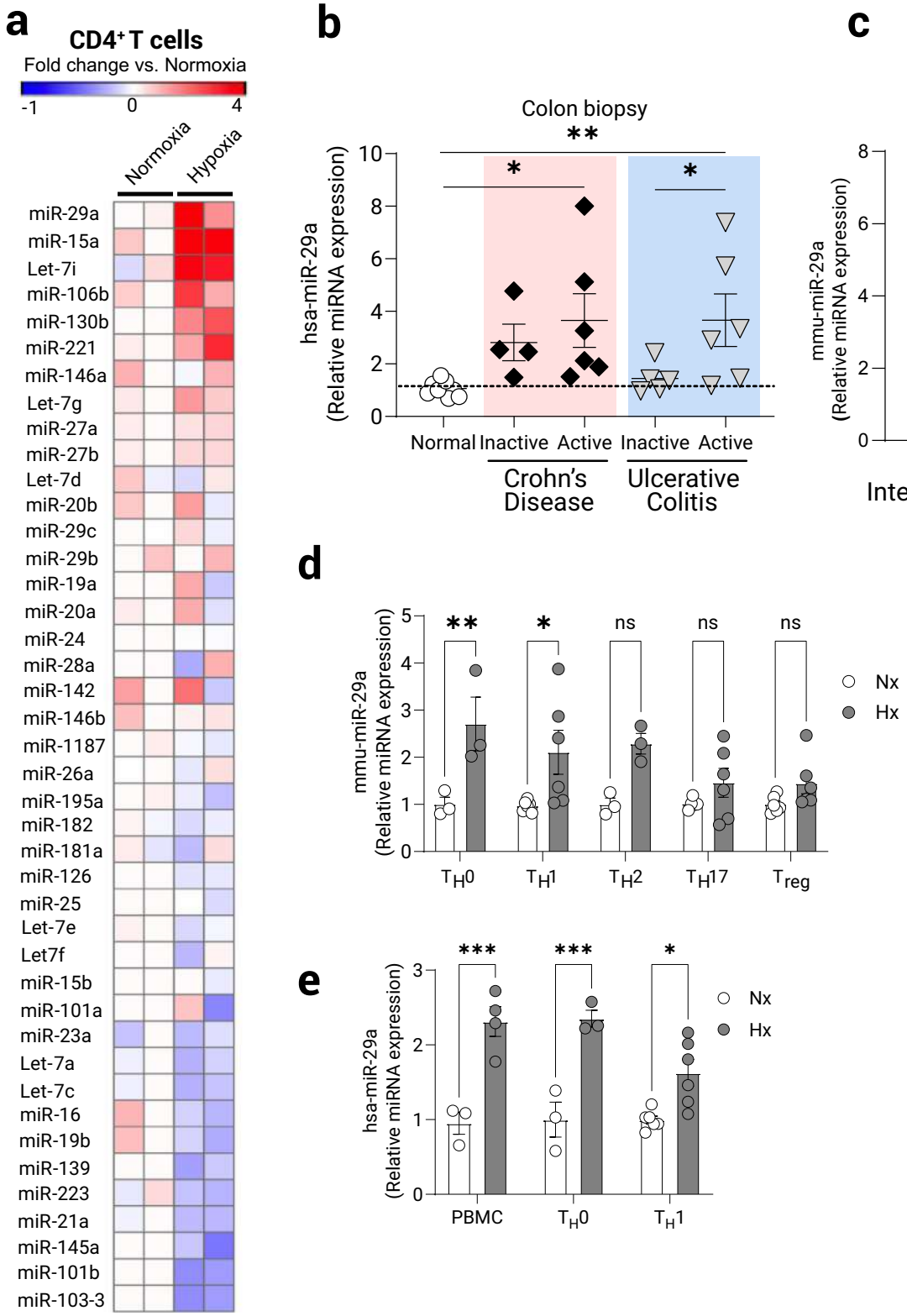

cultured cells under normoxic conditions (Fig. 4a). While normoxic activated cells significantly up-regulated T-bet expression upon activation, hypoxia exposure was not associated with T-bet increases (Fig. 4b). To study the effect of hypoxia on T-bet and its direct target IFNγ, naïve CD4⁺ T cells were differentiated into T_H1 lineage and treated with increasing concentration of DMOG during subsequent activation. Pharmacological stabilization of HIF resulted in a diminished expression of T-bet protein (Fig. 4c) and a dose-dependent decrease of IFNγ release (Fig. 4d). Exposure of CD4⁺ T_H1 T cells to ambient hypoxia over 24 h was associated with attenuated T-bet protein expression following T cell receptor stimulation (Fig. 4e), and a diminished cytokine release (Fig. 4f). Upon transfecting miR-29a inhibitor (antisense) into T cells, the hypoxia-mediated repression of T-bet in proliferating T cells was no longer observed (Fig. 4g, h). Conversely, T cells transfected with miR-29a mimetic downregulate T-bet upon in vitro activation under normoxia compared to control-transfected cells (Fig. 4i).

Fig. 2 | Specific induction of miR-29a in CD4⁺ T cells following experimental hypoxia. Primary naïve CD4+ T cells were isolated from spleens and MLN of C57BL/6J/6J mice and cultured ex vivo for 8 h with TCR stimulation (anti-CD3/28) in either normoxia (21% O_2) or hypoxia (1% O_2). RNA was prepared and assayed using custom limited-target T cell Q-PCR microRNA array (Qiagen). **a** Heat-map representing respective increased and decreased T cell-expressed miRNAs following treatment. Fold change over the average of two normoxia samples is depicted as color change ($n = 2$/group). **b** Assessment of miR-29a expression by Q-PCR in colon biopsies from patients with inflammatory bowel disease. Patient characteristics included in Supplementary Table 1, ($n = 4$–10 patients/group, one-way ANOVA). **c** Normal mouse colon tissue was fractionated into intestinal epithelial cells (IEC) and lamina propria cells (LP) and baseline levels of miR-29a were assessed using Q-PCR, ($n = 4$, two-tailed T test). **d** Primary naïve CD4+ T cells were isolated from spleens of C57BL/6J/6J mice and cultured ex vivo under helper T cell polarizing conditions with rmIL-2 and anti-CD3/anti-CD28 stimulation for 3 days, then washed and rested for 48 h, followed by 8 h stimulation (anti-CD3/28) in either normoxia (21% O_2) or hypoxia (1% O_2). miR-29a expression was assessed by Q-PCR ($n = 3$–6, two-way ANOVA). **e** Primary human CD4+ T cells were isolated from peripheral blood of healthy volunteers and cultured similarly as mouse CD4+ T cells but with only T_H0 and T_H1 specific stimuli. miR-29a expression was assessed by Q-PCR following TCR-stimulation under normoxia or hypoxia for 8 h, ($n = 3$–5, two-way ANOVA). Male and female mice used as cell donors in (**a**, **c**–**e**). Data expressed as mean ±S.E.M., $^*p < 0.05$, $^{**}p < 0.01$, $^{***}p < 0.001$ vs. counterparts.

This data points to a direct role for hypoxia-inducible miR-29a in the regulation of T_H1 master transcription factor T-bet.

Considering the observations above we hypothesized that stabilizing HIF-2α in T cells will lead to protection during colitis by increasing the expression of miR-29a and consequently downregulating the T_H1 response (including and not limited to T-bet induction and IFNγ release) and in turn, diminish the proliferation of pathogenic T cells. For this purpose, we challenged mice with T cell-intrinsic stabilized HIF-2α (*LSL-HIF2dPA Lck Cre*⁺) with 2,4,6-Trinitrobenzenesulfonic acid (TNBS) which leads to a T_H1-mediated colitis. As anticipated, T cells from the mesenteric lymph node (MLN) in colitic mice with stabilized HIF-2α expression failed to up-regulate T-bet protein (Fig. 4j and Supplementary Fig. 2a). Indeed, the *LSL-HIF2dPA Lck Cre*⁺ mice displayed significantly attenuated colitis as indicated by comparatively diminished tissue damage (Fig. 4k) and lower histological scores of colon injury (Fig. 4l and Supplementary Fig. 2b). Taken together, our results provide evidence that the increased miR-29a expression in response to either hypoxia or pharmacological HIF stabilization in vitro, or in a genetic mutation that leads to HIF-2α stabilization in vivo, allows for a coordinated reduction in T_H1 responses during colitis.

T cell-intrinsic HIF-2α dampens T_H1-mediated colitis

As the HIF-2α stabilization in T cells and the consequent modulation of miR-29a expression affects T-bet expression in T_H1 T cells, we wondered about the physiological role of HIF-2α deficiency in the transfer colitis model and the TNBS model. Isolated $CD4^+CD45RB^{high}$ T cells from *Hif-2α$^{loxP/loxP}$ Lck Cre*⁺ mice and littermate controls were transferred into *B6.RAG1-/-* mice. Host animals receiving *Hif-2α*-deficient T cells exhibited significant weight loss compared to control mice (Fig. 5a). At fulminant disease (8 weeks post-transfer), colons were removed and assessed for different measures of disease outcomes. Consistent with a protective role for T cell-intrinsic HIF-2α, we observed significantly higher colon weight-to-length (W/L) ratio in *Hif-2α$^{loxP/loxP}$ Lck Cre*⁺ T cell recipients compared to control mice indicating increased severity of colonic inflammation (Fig. 5b). Mice who received *Hif-2α*-sufficient $CD4^+CD45RB^{low}$ T cells were completely protected from weight loss and colonic inflammation due to the presence of T_{reg} cells in the $CD45RB^{low}$ fraction[46,47] (Fig. 5a, b) and developed no marked colon inflammation (Fig. 5c, d). Adoptive transfer of naïve $CD4^+$ T cells from *Hif-2α$^{loxP/loxP}$ Lck Cre*⁺ and *Lck Cre*⁺ controls (to account for the effect of the *Cre*) resulted in enhanced weight loss (Supplementary Fig. 3b) and colonic inflammation in recipients of HIF-2α deficient cells (Supplementary Fig. 3c). Adoptively transferred *Hif-2α*-deficient T cells in MLN showed increased expression of T-bet (Supplementary Fig. 3d), but no significant differences were noted in expression of IL-17A (Supplementary Fig. 3e). Histological scores were significantly elevated in the recipients of naïve *Hif-2α*-deficient T cells (Fig. 5c), and representative histological colon preparations showed increased recruitment of leukocytes together with pronounced epithelial damage (Fig. 5d). Similarly, disease severity index from day 18-36 were significantly elevated in the recipients of *Hif-2α*-deficient T cells (Supplementary Fig. 3a). T cells isolated from the mesenteric lymph nodes of mice receiving *HIF-2α*-deficient $CD4^+CD45RB^{high}$ T cells showed increased activation of IFNγ and T-bet (Fig. 5e and Fig. 5f, respectively), consistent with the existence of a unique regulatory pathway for T_H1 T cell modulation by HIF-2α-miR-29a axis which works to restrain T_H1 activation during colitis.

Next, *Hif-2α$^{loxP/loxP}$ Lck Cre*⁺ mice together with littermate *Hif-2α$^{loxP/loxP}$ Lck Cre*⁻ controls were sensitized and subsequently challenged with TNBS and, in line with our in vitro data, $CD4^+$ T cells isolated from the mesenteric lymph nodes of mice with a T cell-specific *Hif-2α* deletion displayed elevated expression of T-bet (Fig. 5g) and increased production of IFNγ (Fig. 5h). Heightened histological inflammatory scores indicated significantly exacerbated colitis in *Hif-2α$^{loxP/loxP}$ Lck Cre*⁺ but not in *Hif-2α$^{loxP/loxP}$ Lck Cre*⁻ littermate mice (Fig. 5i). Representative colon micrographs shown in Fig. 5j illustrate increased inflammatory damage in *Hif-2α$^{loxP/loxP}$ Lck Cre*⁺ animals. Taken together, these studies demonstrate that HIF-2α stabilization can restrain T cell inflammatory phenotype, while HIF-2α deficiency in T cells leads to exacerbated disease in mice; therefore, providing a crucial link between inflammatory hypoxia and T lymphocytes in the context of IBD.

Functional role of miR-29a in $CD4^+$ T cells

To study the specific role of miR-29a in T cells, we used previously described mice with a "floxed" miR-29a locus[33] to generate *miR-29a$^{loxP/loxP}$ Lck Cre*⁺ mice and used *miR-29a$^{loxP/loxP}$ Lck Cre*⁻ littermates as experimental controls (details of strain generation in Materials and Methods). T cell-specific deletion of *miR-29a* was confirmed in the total thymocytes (Supplementary Fig. 4a) and in the peripheral naïve $CD4^+$ T cells transiently stimulated under normoxia and hypoxia (1% O_2) with anti-CD3/CD28 antibodies (Fig. 6a). Additionally, *Lck Cre*⁺-derived $CD4^+$ T cells were compared to *miR-29a$^{loxP/loxP}$ Lck Cre*⁺ cells and found to also significantly upregulate miR-29a under hypoxia (Supplementary Fig. 4b). Following activation for 6 h, *miR-29a*-deficient T cells showed increased levels of T-bet mRNA under normoxia and hypoxia (Fig. 6b), with significantly higher expression of IFNγ mRNA as compared to *miR-29a*-sufficient T cells (Fig. 6c). Fully differentiated *miR-29a*-deficient $CD4^+$ T_H1 T cells produced significantly more IFNγ mRNA than controls during 8 h activation with anti-CD3/CD28 under normoxic conditions (Fig. 6d and Supplementary Fig. 4d).

To establish a role for miR-29a in T cells during intestinal inflammation we performed adoptive transfer of naïve $CD4^+$ $CD45RB^{high}$ T cells derived from *miR-29a*-sufficient (*Lck Cre*+) and deficient (*miR-29a$^{loxP/loxP}$ Lck Cre*⁺) mice into *B6.RAG1-/-* recipients. Unexpectedly, both groups displayed similar weight loss scores (Supplementary Fig. 4e). We then hypothesized that T cell differentiation into effector subsets may be impaired in the absence of miR-29a, and to test this we prepared in-vitro skewed T_H1 T cells and adoptively transferred them into *B6.RAG1-/-* recipients. At 9 weeks post transfer mice receiving *miR-29a*-deficient T cells lost significantly less weight (Fig. 6e), although their colon inflammatory scores remained comparable to the controls (Fig. 6f). Both groups displayed similar inflammatory changes in the colon (Fig. 6g). Interestingly, analysis of T cells from the mesenteric

https://doi.org/10.1038/s41467-024-52113-y

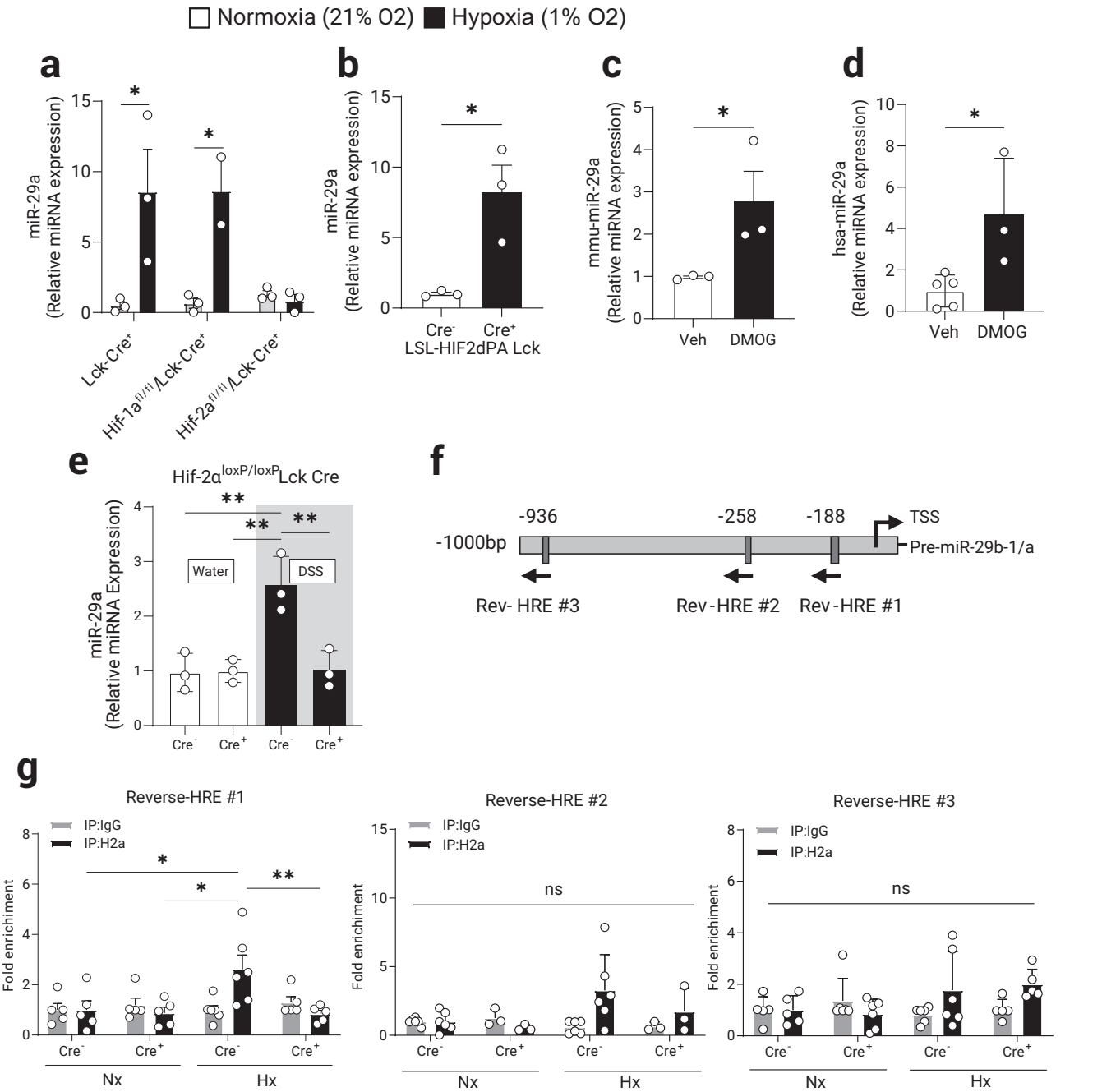

Fig. 3 | HIF-2α mediates the induction of miR-29a in CD4⁺ T cells during hypoxia. Primary mouse naïve CD4⁺ T cells were isolated from spleens and MLN of control (*Lck-Cre⁺)* or mice with a selective HIF-1α or HIF-2α deficiency in T cells. Isolated CD4⁺ T cells were cultured ex vivo for 8 h stimulation with TCR (anti-CD3/28) in either normoxia (21% O_2) or hypoxia (1% O_2). **a** miR-29a induction by hypoxia is absent in *Hif-2α*-deficient CD4⁺ T cells, ($n = 2–3$, two-way ANOVA). **b** miR-29a is significantly induced in primary CD4⁺ T cells isolated from *Hif-2α*-over-expressing mice (*LSL-HIF2dPA Lck Cre⁺*) cultured ex vivo for 8 h stimulation with TCR stimulation ($n = 3$, two-tailed *T* test). Pharmacologic stabilization of HIF-2α with DMOG treatment (1 mM) induced miR-29a in: (**c**) primary CD4⁺ T cells from WT (B6) mice ($n = 3$, one-tailed *T* test) and, (**d**) CD4⁺ T cells isolated from PBMCs of healthy human volunteers ($n = 3–5$, two-tailed *T* test). *Hif-2α$^{loxP/loxP}$ Lck Cre⁺* and *Hif-2α$^{loxP/loxP}$ Lck Cre⁻* mice were treated with two rounds of 3% DSS in drinking water for 5 days with 2 weeks of water in between treatments to induce chronic colitis. **e** Quantification of miR-29a expression in the total mouse colon tissue, ($n = 3$, two-way ANOVA). **f** Schematic representation of murine *miR-29b1-a* promoter with 3 most proximal putative Hypoxia Responsive Elements (HRE) indicated. More distant putative HREs (4) were omitted. **g** Chromatin Immuno-Precipitation (ChIP) was performed to assess in vivo DNA-protein interactions at the proximal promoter sequences in primary CD4+ T cells from *Hif-2α$^{loxP/loxP}$ Lck Cre⁺* and *Cre⁻* mice cultured ex vivo for 8 h with TCR stimulation (anti-CD3/28) in either normoxia (21% O_2) or hypoxia (1% O_2) as per *Methods* ($n = 6$, two-way ANOVA). Male and female mice used in (**a**–**d**, **g**), male mice used in (**e**). Data expressed as Mean ±S.E.M from 2 polled independent experiments., $^*p < 0.05$, $^{**}p < 0.01$.

lymph nodes showed that effector T cell differentiation is affected by the loss of miR-29a (Fig. 6h). While *miR-29a*-deficient T cells efficiently retained their T_H1 lineage commitment and produced high amounts of IFNγ (Fig. 6i) with notably higher survival rate under hypoxia (Supplementary Fig. 4c), the *miR-29a*-sufficient T cells were more proficient differentiating into IL-17A-producing T cells (Fig. 6j). Indeed, purified CD4⁺ miR-29a-deficient T cells skewed in-vitro towards T_H17 show diminished survival (Supplementary Fig. 4f and Supplementary Fig. 4g) and limited IL-17A production under hypoxia (Supplementary Fig. 4h). The loss of T_H1 identity and differentiation into IL-17A⁺ T cells within

https://doi.org/10.1038/s41467-024-52113-y

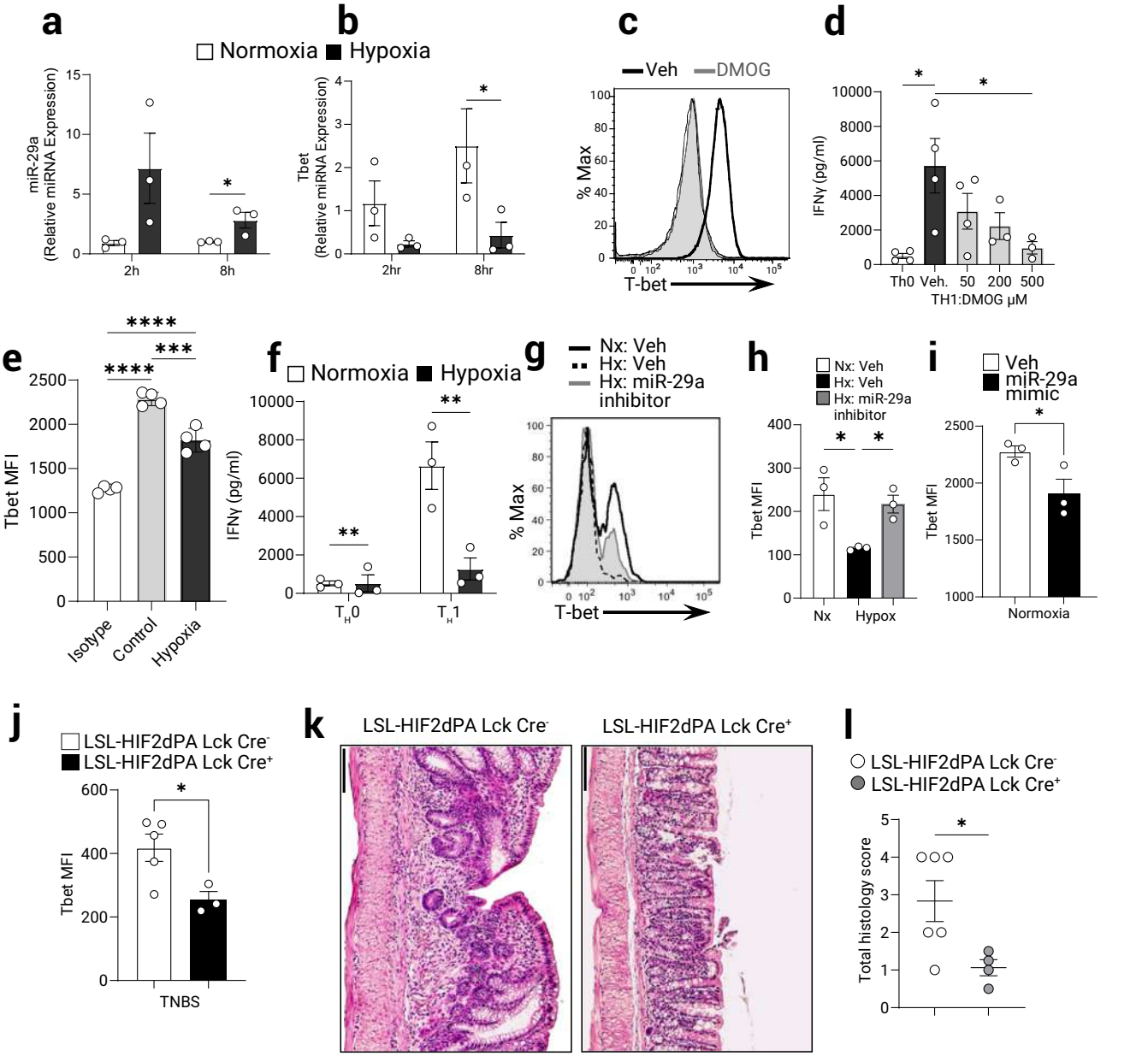

Fig. 4 | T-bet expression in CD4⁺ T_H1 T cells is specifically repressed during hypoxia via miR-29a. MicroRNA-29a targets T-bet expression in vitro and in vivo. CD4⁺ T cells were isolated from spleens and MLN of WT (B6) mice and cultured ex vivo with anti CD3/CD23 for indicated time under normoxia (21% O_2) or hypoxia (1% O_2). **a** mRNA expression of miR-29a in CD4⁺ T cells was measured by Q-PCR ($n = 3$, one-tailed T test), and **b** mRNA expression of T-bet was measured by Q-PCR following 2 h and 8 h in either normoxia (21% O_2) or hypoxia (1% O_2), ($n = 3$, pooled 2 experiments, two-way ANOVA). CD4⁺ T cells were isolated from spleens and MLN of WT (B6) mice and cultured ex vivo under T_H1 polarizing conditions. Differentiated T_H1 T cells were stimulated with anti-CD3/anti-CD28 under normoxia (21% O_2) or hypoxia (1% O_2) for 1 day. **c** T-bet protein was measured by flow cytometry in T_H1 T cells untreated or treated with DMOG (conc. 500 μM). Representative plot shown. **d** IFNγ secretion from T_H1 T cells treated with DMOG was assessed by ELISA ($n = 3$–4, one-way ANOVA). **e** T-bet protein expression was measured by flow cytometry in cells stimulated for 24 h under normoxia or hypoxia ($n = 4$, one-way ANOVA). **f** IFNγ secretion in T_H0 or T_H1-skewed cells was assessed by ELISA on day 3 ($n = 3$, 2-way ANOVA). T-bet protein expression measured by flow cytometry in T_H1 differentiated CD4⁺ T cells transfected with specific mi-29a inhibitor (**g**, **h**) or miR-29a mimetic (**i**) and activated with anti CD3/CD28 in normoxia or hypoxia for 48 h. **g** Representative flow cytometry profile of T bet expression. **h** Quantitation of Tbet fluorescence from (**g**) (n = 3, one-way ANOVA). **i** Quantitation of Tbet in cells transfected with miR-29a mimic and analyzed by flow cytometry ($n = 3$, one-tailed T test). T_H1 colitis was induced in *LSL-HIF2dPA Lck Cre*⁺ mice and controls by epicutaneous skin sensitization followed by rectal gavage with TNBS as per Materials and Methods. **j** T-bet protein expression in gated CD4⁺ T cells purified from lamina propria was measured by flow cytometry ($n = 3$–5, two-tailed T test). **k** Representative micrographs of TNBS-treated colons from *LSL-HIF2dPA Lck Cre*⁺ or *Cre*⁻ littermate controls stained with H&E, bar = 100 mm. **l** Histological scores from *LSL-HIF2dPA Lck Cre*⁺ or *Cre*⁻ littermate controls following TNBS trial ($n = 4$–6, two-tailed T test). Male and female mice used in (**a**–**l**). Data expressed as Mean ± S.E.M, $^*p < 0.05$, $^{**}p < 0.01$ vs. indicated.

the hypoxic intestinal environment in the transfer colitis model has been described previously[48], and a report by Leppkes et al.[49] identified the highly pathogenic role for IL-17A⁺ T cells in the transfer colitis model which results in a higher disease severity than IFNγ⁺ T cells alone. We conclude that in CD4⁺ T cells deletion of miR-29a relieves the restraint on T-bet expression and leads to better retention of T_H1 identity and higher IFNγ production concomitant with an impairment in IL-17A production resulting in a diminished disease severity.

To further study the role for miR-29a in T_H1 T cells during intestinal inflammation we exposed mice with T cell-specific *miR-29a* deletion to

https://doi.org/10.1038/s41467-024-52113-y

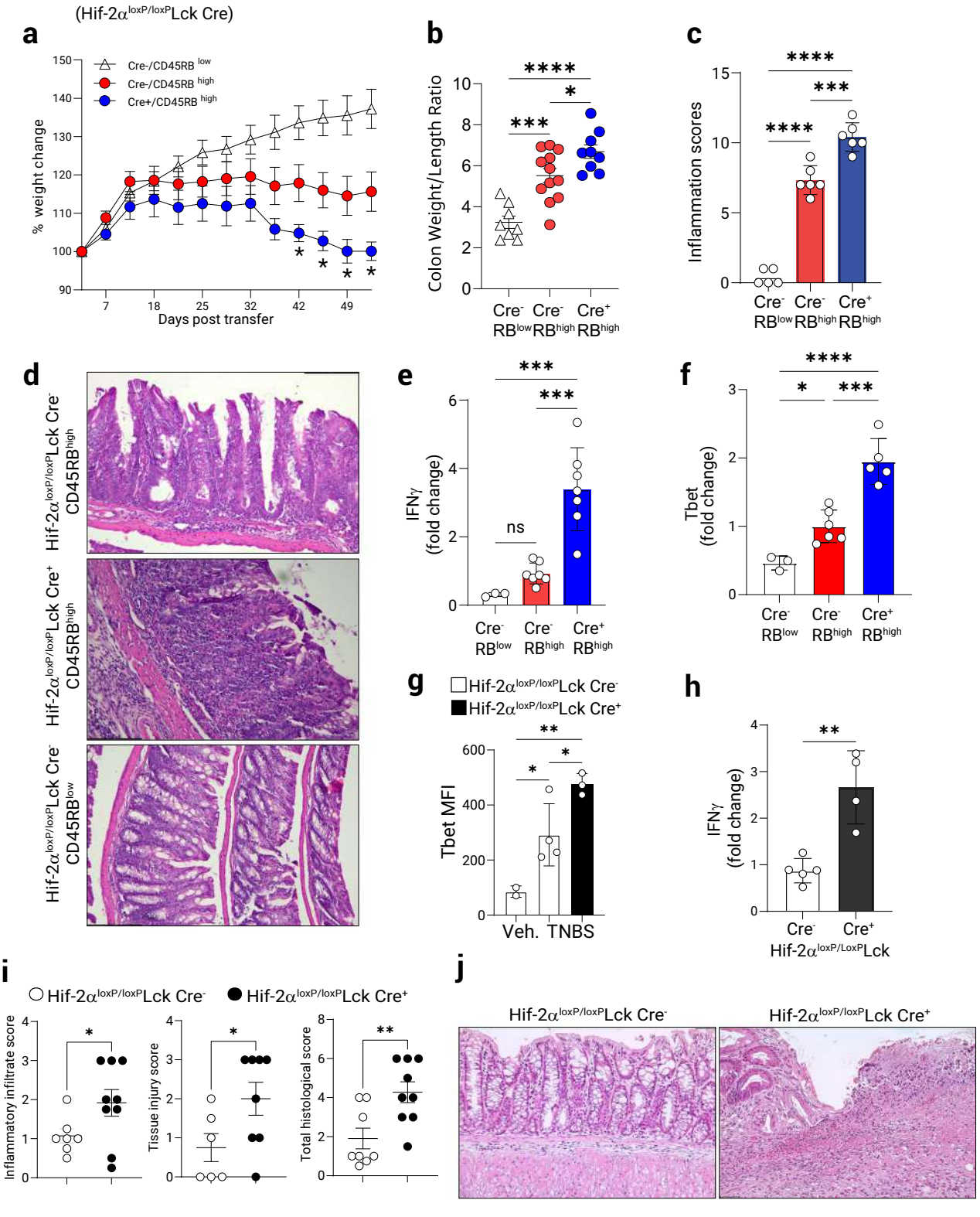

TNBS colitis. Consistent with a functional role of miR-29a in suppressing a Th1 response, *miR-29a*$^{loxP/loxP}$ *Lck Cre*$^{+}$ mice lost weight at a higher rate and took longer to regain it (Fig. 6k) while their colons appeared significantly shortened compared to the littermate controls (Fig. 6l). Moreover, cumulative disease scores that account for the onset and degree of symptoms were significantly increased in animals with T cell-specific *miR-29a* deletion (Supplementary Fig. 5a). Colonic explants from these mice released significantly more IFNγ upon 20 h ex vivo culture, indicating higher inflammation (Fig. 6m). Importantly, flow cytometric analysis of *miR-29a*-deficient CD4^{+} T lymphocytes isolated from the lamina propria of TNBS-treated mice showed increased expression of T-bet protein compared to their littermate controls (Fig. 6n). Histological scores (Fig. 6o) and representative histological images (Fig. 6p) demonstrated a more severe inflammation, more pronounced crypt erosion and lymphocyte infiltration into the mucosal layer in the *miR-29*$^{loxP/loxP}$ *Lck Cre*$^{+}$ but not *Cre*$^{-}$ littermate mice. To

Fig. 5 | T cell-intrinsic HIF-2α regulates T cell function in Colitis. Chronic T cell-mediated colitis was induced in B6.B6.RAG1−/− mice by intraperitoneal adoptive transfer of naïve $CD4^+$ $CD45RB^{high}$ or $CD45RB^{low}$ T cells (0.5×10^{6}/ animal) derived from *Hif-2α$^{loxP/loxP}$ Lck Cre$^+$* or *Cre$^-$* animals. **a** Weight change during the course of colitis ($n = 8–10$, 2-way ANOVA, Cre- vs. Cre+). **b** Colon weight/length ratio at fulminant disease ($n = 9–12$, one-way ANOVA). **c** Histological preparations of colons stained with H&E were scored for total inflammation (as per *Methods, (*$n = 5–6$, one-way ANOVA). **d** Representative micrographs of colons at day 56 post-transfer, scale bar: 131.4 mm. Mesenteric lymph node $CD4^+$ T cells were purified from adoptively transferred mice and total RNA was assayed by Q-PCR for: **e** IFNγ mRNA expression ($n = 3–7$, one-way ANOVA). **f** T-bet mRNA expression. Gene expression in (**e**, **f**) was normalized to 18s rRNA. ($n = 3–6$, one-way ANOVA). T_H1 colitis was induced in *Hif-2α$^{loxP/loxP}$ Lck Cre$^+$* or *Lck Cre$^+$* control mice by the epicutaneous skin sensitization and subsequent rectal gavage with TNBS. At the time of necropsy mesenteric node lymphocytes were assessed by flow cytometry. **g** T-bet mean fluorescence intensity (MFI) in $CD4^+$ T cells (gated on live CD3+, $n = 3–4$, one-way ANOVA). **h** IFNγ expression in mesenteric node lymphocytes was assayed by Q-PCR ($n = 4–5$, two-tailed *T* test). **i** Histological indices including leukocyte infiltration, tissue injury and total inflammation in the course of colitis ($n = 6–9$, one-tailed *T* test). **j** Representative micrographs from *Lck Cre$^+$* controls or *Hif-2α$^{loxP/loxP}$ Lck Cre$^+$* mice 7 days post-challenge, scale bar 100 mm. Male recipients and mixed male/female donors used in (**a**–**f**), male and female mice used in (**g**–**j**). Data expressed as Mean ± S.E.M, $*p < 0.05$, $**p < 0.01$, $***p < 0, .001$. vs. indicated.

eliminate strain bias, similar experiments were performed in *miR-29$^{loxP/loxP}$ Lck Cre$^+$* and *Lck Cre$^+$* mice which displayed comparable weight loss pattern (Supplementary Fig. 5b), colon shrinkage and histopathology changes (Supplementary Fig. 5c, d). IFNγ production in cell culture of naïve and differentiated T_H1 T cells from *miR-29$^{loxP/loxP}$ Lck Cre$^+$* was significantly higher than *Lck Cre$^+$* controls (Supplementary Fig. 5e), while production of another proinflammatory cytokine, TNFα, was not significantly changed in the context of T cell intrinsic miR-29a deficiency in vitro (Supplementary Fig. 5f, Supplementary Fig. 5g) or in vivo (Supplementary Fig. 5h). Taken together, these studies indicate that T cell intrinsic deletion of *miR-29a* is associated with enhanced hyperactivity in vitro, and concomitant increases in T_H1-mediated activation and proliferation during experimental colitis.

Nanoparticle delivery of miR-29a attenuates colitis in mice

Having demonstrated a functional impact of miR-29a deletion in T cells towards unrestrained T-bet and IFNγ output resulting in enhanced inflammatory phenotype, we next pursued studies to address a potential therapeutic application of miR-29a overexpression. Small molecules targeted at aberrant inflammation pathways are the focus of intense investigation both for IBD diagnosis and treatment, and the first small-interfering RNA (siRNA) was recently approved by the FDA for the treatment of amyloidosis[50]. Therefore, we pursued studies to investigate the efficacy of utilizing miR-29a mimetic as a therapeutic intervention during experimental colitis.

In order to confirm that mucosa-homing T cell are able to retain microRNA mimetics, we intraperitoneally injected Cy3-labeled and liposome-packaged microRNA (tracer miRNA with no biological activity) into colitic C57BL/6J/6J mice that were previously challenged with TNBS. Mesenteric lymph nodes were subsequently isolated and assayed by flow cytometry. We observed accumulation of Cy3-positive $CD4^+$ T cells in the mesenteric lymph node within 5 h post-injection (Supplementary Fig. 6a, b), which diminished over time indicating cell migration and microRNA turnover (Supplementary Fig. 6c).

To test the efficacy of miR-29a therapy during inflammation synthetic murine miR-29a mimetics were delivered to mice in a lipid emulsion of nanoparticles (iv, chosen as the preferred method requiring less handling time for the mimetic prior to injection) on days 1 and 3 post-TNBS administration[51]. As a relevant control, we used a corresponding miRNA that is restrictively expressed in *C. elegans* nematode [(Cel-miR-239b) (miRIDIAN microRNA Mimic Negative Control #2, Horizon Discovery Biosciences Ltd.)]. The miR-29a mimetic treatment (Fig. 7a) markedly attenuated intestinal pathology compared to a control treatment as indicated by decreased total disease index which is comprised of the inflammatory index and the injury index (Fig. 7b). Representative histological slides show significantly diminished lymphocyte infiltration and a lesser damage to the colonic lining in the mimetic-treated group (Fig. 7c), (Cel-miR-239b: $p < 0.05$). Mimetic treatment further resulted in a significant concomitant attenuation of colonic T-bet and IFNγ mRNA levels, indicating that it affects the functional status of $CD4^+$ T cells in vivo (Fig. 7d, e respectively).

To extend our studies into the therapeutic effects of miR-29a mimetics, we next pursued a spontaneous-onset ileitis model using *TNF$^{\Delta ARE/+}$* mice which is a mouse model of Crohn's disease (CD) in which $CD4^+$ effector T cells play a central role[52]. These mice express a single copy of mutated *TNFα* causing over-stabilization of TNFα mRNA and systemically elevated TNFα protein, eventually leading to a spontaneous development of chronic transmural ileitis resembling CD in humans. Mimetic treatment of *TNF$^{\Delta ARE/+}$* mice consisted of four intravenous injections during active disease period (Fig. 7f). Upon conclusion of treatment with miR-29a mimetic, *TNF$^{\Delta ARE/+}$* mice were showing reduced number of IFNγ$^+$ $CD4^+$ T cells in the MLN as compared to control-mimetic treated mice (Fig. 7g), and these animals developed significantly diminished histological changes in the ileum (Fig. 7i, j). These results establish miR-29a as a potential therapeutic agent in the treatment of IBD that may present a viable clinical option in human patients in the future.

Collectively, these experiments demonstrate that liposome-packaged miR-29a mimetic is retained by $CD4^+$ T cells in colitis which may lead to a significant reduction of disease outcomes in multiple IBD models. While we cannot exclude the miR-29a mimetic exerting activity in other cell types during our treatment, miR-29a appears to function as a bona fide regulator of T_H1 $CD4^+$ T cell activity during experimental colitis and is a potential therapeutic target in the treatment of IBD.

Discussion

In the present study, we demonstrate that HIF signaling via miR-29a in T_H1 T cells is essential for limiting inflammation during colitis. Dysregulated activation and excessive cytokine production by lymphocytes, in particular by $CD4^+$ T cells, has been implicated in driving aberrant inflammation observed during IBD. The molecular machinery coordinating the $CD4^+$ T cell function in IBD is not yet fully understood. Our findings highlight a critical and previously undefined role for HIF-2α in regulating the inflammatory environment within the intestine. We show that inflammatory hypoxia resulting from colitis and its resultant HIF-2α signaling coordinates increased expression of miR-29a in the T cells. This HIF-2α enhancement of miR-29a in turn, represses select T_H1 responses including T-bet and IFNγ in $CD4^+$ T cells. Mice with a T cell deficiency in HIF-2α display heightened experimental colitis scores and enhanced T_H1 markers in T cells. Mice with a T cell intrinsic deficiency of miR-29a show enhanced colitic profiles in T_H1-mediated colitis with concomitantly increased T-bet expression and cytokine production combined with enhanced mucosal injury score. Enhanced T_H1 phenotype of *miR-29a*-deficient T cells leads to impaired T_H17 differentiation in the inflamed mucosa in the transfer colitis model. Furthermore, we demonstrate that nanoparticle delivery of miR-29a mimetics can repress bowel inflammation and attenuate T_H1 T cell activity in disease.

Recent studies highlighted a decline in oxygen availability during periods of inflammation within the intestinal mucosa, which is a result of increased oxygen consumption by resident mucosal cells and the infiltrating leukocytes. Oxygen deprivation leads to cellular responses that help in adaptation involving activation of hypoxia-inducible factors HIF-1α and HIF-2α in a cell type-specific manner. The importance of HIF

https://doi.org/10.1038/s41467-024-52113-y

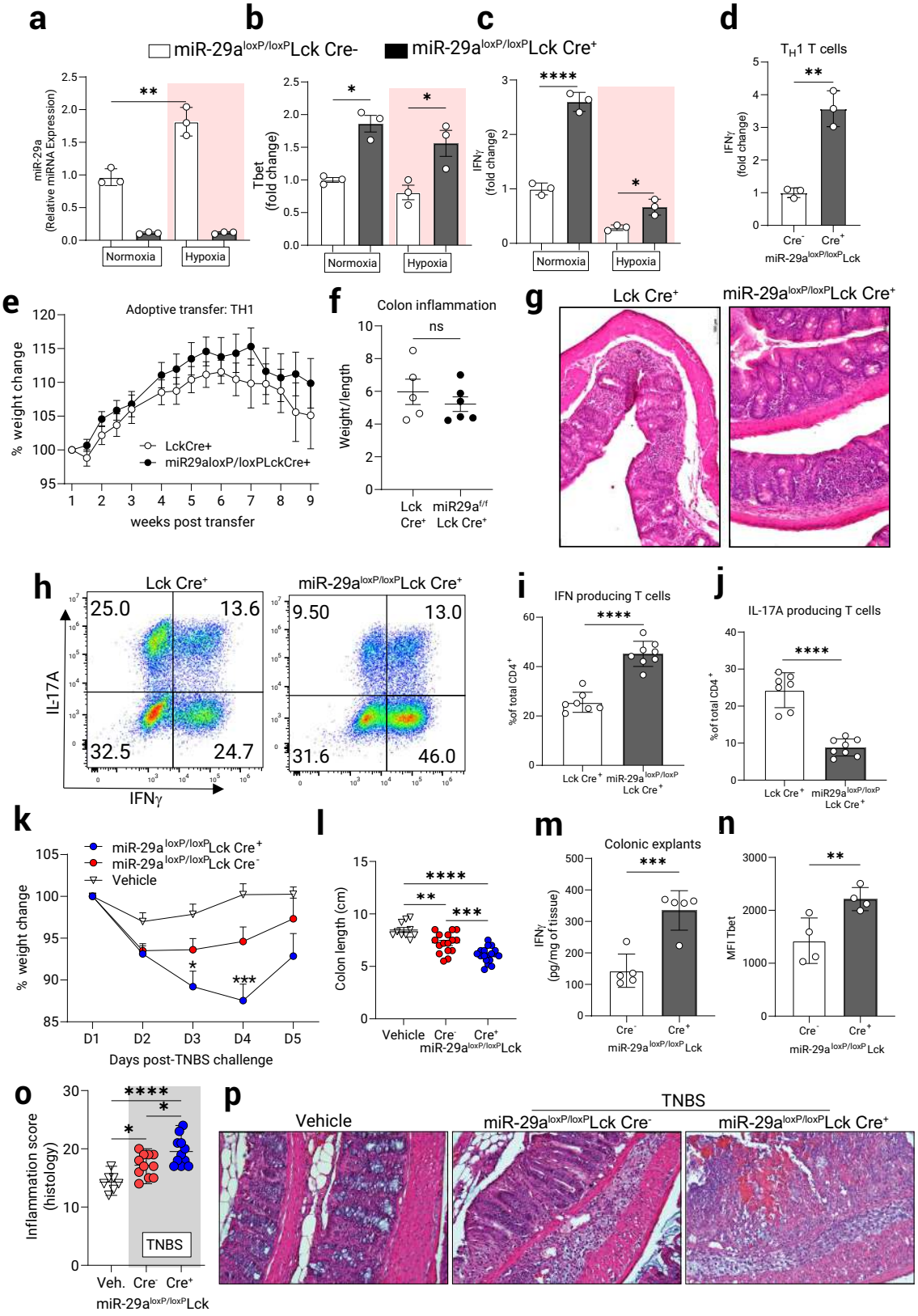

signaling during intestinal and systemic inflammation has been studied in the context of epithelial cells and T cells[3,53–56]. Similarly, previous studies have addressed the essential role of microRNAs in cellular programs aimed towards resolution of tissue inflammation[57–59]. Our work adds to these findings by demonstrating that T cell-specific HIF-2α mediated miR-29a enhancement is important to limit lymphocyte activation in colitis. The exact function of HIF-2α in colitis appears to be strictly cell-specific as earlier reports show that deletion of HIF-2α in the intestinal epithelium is protective in colitis and prevents colon cancer initiation[60,61]. Our data points to a disease-protective effect of HIF-2α signaling in CD4$^+$ T cells which are reprogrammed by the hypoxic environment of inflamed intestine to limit their proliferation and

Fig. 6 | T cell-intrinsic miR-29a regulates T cell function in vitro and in vivo. Naïve CD4$^+$ T cell were purified from *miR-29a$^{loxP/loxP}$ Lck Cre$^+$* or *Cre$^-$* mice and stimulated with anti-CD3/anti-CD28 for 5 h in normoxia (21% O_2) or hypoxia (1% O_2). Q-PCR assays were employed to measure: (**a**) microRNA expression of miR-29a, ($n = 3$, two-way ANOVA). **b** mRNA expression of T-bet, **c** mRNA expression of IFNγ. (**b**, **c**: $n = 3$, repeated 2 times, two-way ANOVA). **d** mRNA level of IFNγ in T_H1-skewed T cells grown in vitro for 3 days and then re-stimulated with anti-CD3/anti-CD28 for 8 h, ($n = 3$, two-tailed *T* test). 7-week-old B6.RAG1−/− recipient mice were adoptively transferred with 10^6 in-vitro differentiated CD4$^+$ T_H1 T cells from *Lck Cre$^+$* and *miR-29a$^{loxP/loxP}$ Lck Cre$^+$* mice and weight changes were recorded twice per week. **e** Weight change chart with transient weight gain followed by continuous weight loss in the course of colitis development, ($n = 7–8$). **f** Colon inflammatory score (colon weight/length), ($n = 6$, n.s). **g** Representative micrographs of H&E staining in the colon show infiltration of lymphocytes into the intestinal epithelium in *Lck Cre$^+$* and *miR-29a$^{loxP/loxP}$ Lck Cre$^+$* mice. Original magnification ×20, scale bar: 100 mm. Mesenteric lymph node (MLN) cells were isolated and re-stimulated for 5 h in vitro with PMA/Ionomycin in the presence of Brefeldin A, stained for intracellular cytokines and gated on live CD4$^+$ lymphocytes. **h** Representative plots for each mouse group are shown. **i** Proportion of IFNγ producing CD4$^+$ T cells in the MLN ($n = 7–8$, two-tailed *T* test). **j** Proportion of IL-17 producing CD4$^+$ T cells ($n = 7–8$, two-tailed *T* test. T_H1 colitis was induced in *miR-29a$^{loxP/loxP}$ Lck Cre$^+$* mice and controls by the epicutaneous skin sensitization and subsequent rectal gavage with TNBS as per Materials and Methods. **k** Weight loss curve, ($n = 8–12$, two-way ANOVA). **l** Colon length in TNBS-challenged mice ($n = 10–18$, one-way ANOVA). **m** Colonic explants were cultured for 24 h and IFNγ release was measured using ELISA, ($n = 5$, two-tailed *T* test). **n** At the time of necropsy, lamina propria lymphocytes (LPL) were purified and CD4$^+$ T cells were assayed by flow cytometry for expression of Tbet protein ($n = 4$, one-tailed *T* test). **o** Histological index of colitis. ($n = 8–11$, One-way ANOVA). **p** Representative micrographs from TNBS-treated *miR-29a$^{loxP/loxP}$ Lck Cre$^+$*, *miR-29a$^{loxP/loxP}$ Lck Cre$^-$* or vehicle -treated mice 5 days post-challenge, scale bar is 100 mm. Male and female mice used in (**a**–**d**, **k**–**p**). Male recipients and mixed male/female donors used in (**e**–**j**). $^*p < 0.05$, $^{**}p < 0.01$, $^{****}p < 0.0001$ vs. indicated, Q-PCR microRNA expression normalized to RNU6B and mRNA expression to 18s rRNA.

cytokine production, therefore limiting their pathogenicity. Understanding the molecular mechanism(s) of hypoxia-driven anti-inflammatory and tissue-protective transcriptional machinery in the infiltrating leukocyte transcriptome is an attractive avenue to target therapeutically.

HIF-1α has been shown to affect the differentiation and function of different T cell subsets under hypoxic and normoxic conditions[62]. Deletion of *Hif-1α* in T cells leads to an anti-inflammatory phenotype with increased production of T_{reg} cells and enhanced animal survival in several inflammatory models in vivo, while negatively impacting T_{reg} differentiation and T_H1-mediated IFNγ release under hypoxia in vitro[3,63]. In contrast, the functional role of HIF-2α in the differentiation and activation of T cells is poorly defined. HIF-2α was shown to regulate differentiation of T_H9 and T_{reg} cells in a microRNA-dependent pathway[20]. In addition, a recent report highlighted an unexpected anti-inflammatory role for HIF-2α in T_{reg} stability: *Hif-2α*-deficient T_{reg} cells have an impaired ability to suppress effector T cells in mouse inflammatory models while making same animals simultaneously resistant to tumor growth[18]. To the best of our knowledge, our study is the first to directly address the role of HIF-2α in T_H1 T cells.

Hundreds of different conserved miRNAs have been identified, however, the role of microRNAs in mucosal immunity and IBD is only beginning to be elucidated[64]. In T cells, the microRNA expression patterns vary among subsets and stages of cellular development[65,66]. Of note, deletion of Dicer specifically in murine T cells results in more IFNγ$^+$ CD4$^+$ T cells[28] and deletion of Drosha throughout the T cell compartment results in spontaneous inflammatory disease due to the presence of more IL-17A$^+$ CD4$^+$ T cells and/or IFNγ$^+$ CD4$^+$ T cells[67]. Collectively, these studies suggest that distinct miRNAs play an essential role in the maintenance of T cell immune homeostasis and immune defense[29,68]. Chief among these, miR-29a, is emerging as a crucial regulator of the adaptive immune system and specifically of the T_H1 CD4$^+$ T cells[31,45]. Global genetic deletion of miR-29a leads to a complex mouse phenotype that manifests with a hematopoietic stem cell deficiency and exhaustion as well as premature attrition of the thymus[25,69]. By acting on T-box binding transcription factor (T-bet) and the IFNγ pathway, miR-29a can suppress the T_H1-helper T cell differentiation pathway, and the deletion of miR-29b leads to impaired T_H1 responses in the mouse model of multiple sclerosis[31,33]. Reducing miR-29a expression using a sponge target during ongoing bacterial infection decreases bacterial burden by enhancing the T_H1 response in mice. Suppressive effect of miR-29a on IFNγ within the thymic epithelium increases the threshold for infection-associated signals and protects against thymic involution[70]. Several signal transduction pathways regulating miR-29 family of miRNAs have been described in the context of specific diseases[71]. For example, a report by Chandiran et al. highlighted the role of Notch-1-mediated miR-29a repression in early T-cell differentiation towards T_H1[72], while others studied the role of AKT-MYC-dependent regulation of miR-29s expression in B cell malignancies[33,73], underscoring the cell type-specific regulation of these miRNAs in lymphocyte biology. While our work focuses specifically on the aspects of miR-29a activation in CD4$^+$T cells by tissue hypoxia, some of the previously identified mechanisms of miR-29a activation may also contribute to the phenotypes observed in our study.

In this report we address a major outstanding knowledge gap: how the expression of the microRNA-29a is regulated in the T cells as a reflection of the physiological conditions in the body during homeostasis and under inflammation. We provide relevant biological context for the hypoxia-mediated coordination of miR-29a activity by hypoxia inducible factor 2a (HIF-2α) in T cells within an inflammatory setting. The inflammatory hypoxia within the diseased intestine initiates tissue-protective response that limits immune hyperactivity. Evidence from several studies suggests that pharmacological activation of HIFs may be protective in intestinal inflammation[74–78] and potentially some of that protective effect is mediated by HIF-dependent micro RNAs. Our genetic deletion data implicates HIF-2α as an enhancer of miR-29a in T cells during intestinal inflammation, while the miR-29a mimetic significantly ameliorates the diseases outcomes. Indeed, a recent study of acute DSS-induced colitis in mice showed that delivering a miR-29a mimetic within the supercarbonate-apatite complexes may alleviate the intestinal pathology in this model, albeit by targeting distinct components of the innate immune response[79] and suggesting additional protective roles for this microRNA. Thus, pharmacologic delivery of miR-29a or stabilization of miR-29a-inducing stimuli (e.g.: T cell-intrinsic HIF-2α) holds promise as a future therapeutic modality for active flares in IBD and a physiologically tailored therapeutic approach to IBD therapies; a welcome alternative to the current broad immune suppressant treatments. The next goal of such deliberate therapeutic interventions will be to improve the delivery routes to specific cellular subsets and to limit non-specific effects of microRNA delivery in the treatment of IBD.

Methods

Mice

C57BL/6J/6J mice were bred in house. HIF-luciferase reporter mice (FVB.*129S6-Gt(ROSA)26Sor$^{tm2(HIF1A/luc)Kael}$*/J, Strain #:006206) [referred to as ODD-luciferase], *Lck Cre* [B6.*Cg-Tg(Lck-cre)^{548Jxm}*/J, Strain #:003802], *Hif-1a$^{loxP/loxP}$*(B6.129-*Hif1a^{tm3Rsjo}*/J, Strain #:007561), *Hif-2α$^{loxP/loxP}$* (*Epas1^{tm1Mcs}*/J, Strain #:008407), *LSL-Hif-2dPA* (*Gt(ROSA)26Sor$^{tm4(HIF-2α*)Kael}$*/J, Strain #:009674) and B6.RAG1-/- (*B6.129S7-Rag1^{tm1Mom}*/J, Strain #:002216) were purchased from Jackson Laboratories (Bar Harbor, ME). Floxed miR-29ab1 (*miR-29a$^{loxP/loxP}$*) mice were a gift from Caroline C. Whitacre[33] and these were subsequently backcrossed to C57BL/6 J/6 J. T cell intrinsic deficient mice were generated by the F_2 progeny of the above floxed strains and *Lck Cre$^+$*. To eliminate strain or microbiota

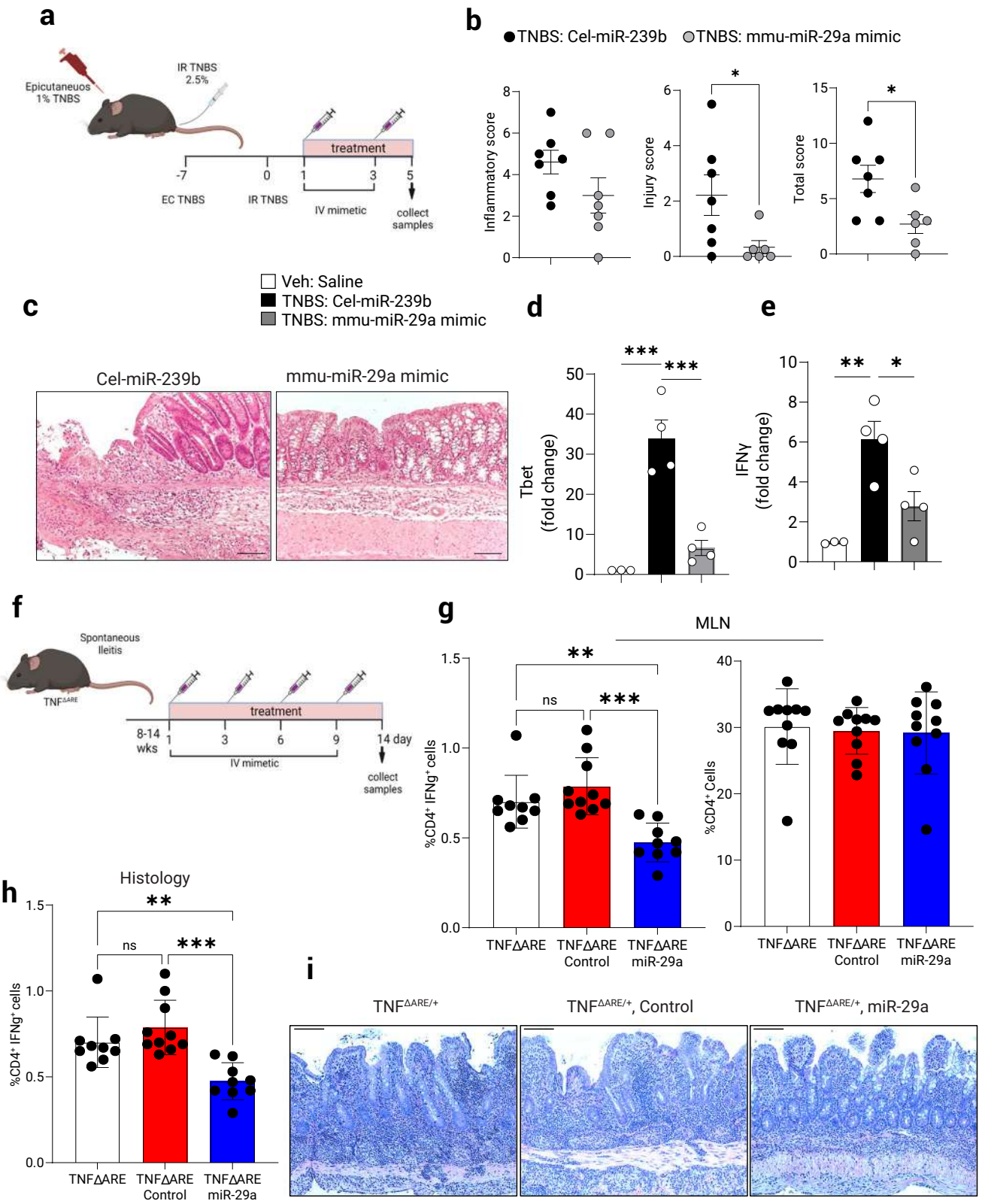

bias, experiments were performed in littermates using Cre$^-$ mice as controls and also in *Lck Cre*$^+$ control mice. Experimental mice used were age- and sex-matched mice and typically between 8 and 12 weeks of age. To generate a sub-strain of ODD-luciferase mice on a *C57BL/6J/6J* background, FVB.*129S6-Gt(ROSA)26Sor*$^{tm2(HIF1A/luc)Kael}$/J were backcrossed with *C57BL/6J/6J* mice for over seven generations. The *B6.129S-Tnf*^{tm2GK1}/*Jarn* strain (*TNF*$^{\Delta ARE/+}$; MGI:3720980) was generated by continuous backcrosses between heterozygous TNF$^{\Delta ARE/+}$ on a mixed background[12] to C57BL/6J6/J mice and kept under specific pathogen-free conditions. Experimental animals were heterozygous for the ΔARE mutation (*TNF*$^{\Delta ARE/+}$) or homozygous wildtype (WT), which served as controls. In this model mice were used between 10-14 weeks of age. All animals were

Fig. 7 | Nanoparticle delivery of a miR-29a mimetic attenuates T_H1-mediated TNBS Colitis. T_H1 colitis was induced in WT mice by TNBS dosing as per Materials & Methods. At 24 h and 72 h post-challenge mice were injected IV with respective mimic microRNA in lipid nanoparticle emulsion (5 μg/mouse). **a** Schematic of experimental design and treatments in TNBS-colitis model. **b** Histological indices of colitis (inflammatory, injury, and total) were assessed 5 days post-TNBS challenge, pooled 2 experiments, ($n = 6–7$, two-tailed T test). **c** Representative H&E micrographs of colons. Scale bar: 100 mm. **d** At the time of necropsy, purified lamina propria lymphocytes were assessed by Q-PCR for. the expression of T-bet mRNA, normalized to 18S rRNA, ($n = 3–4$, one-way ANOVA). **e** Expression of IFNγ mRNA in purified lamina propria T lymphocytes. Data expressed as Mean ±S.E.M from 2 pooled experiments, ($n = 3–4$, one-way ANOVA). $TNF^{\Delta ARE/+}$ mice manifest with spontaneous ileitis. **f** Schematic of miR-29a mimetic treatment schedule of $TNF^{\Delta ARE/+}$ mice. **g** Flow cytometry staining of IFNγ-positive $CD4^+$ T cells and number of $CD4^+$ T cells as a percentage of total MLN cells at the conclusion of experiment, 2 pooled experiments, ($n = 9–10$, one-way ANOVA). **h** Overall histological inflammatory score, 2 pooled experiments, ($n = 13$, one-way ANOVA). **i** Representative H&E micrographs of the ileum in control (untreated), mock-treated and miR-29a mimetic treated mice. Scale bar: 100 mm. Male and female mice used in all experiments. Data expressed as Mean ±S.E.M, $^*p < 0.05$, $^{**}p < 0.01$ vs. indicated. Schematics in (**a**, **f**) were created with BioRender.com.

housed under a 12-hour light/12-hour dark cycle in an animal facility under specific pathogen-free conditions. All mice were handled and euthanized in a humane manner (euthanasia by overdose injection with pentobarbital). Animal procedures were approved by the Institutional Animal Care and Use Committee at the UT Health Science Center in Houston and the University of Colorado, Denver. In conducting research using animals, the investigators adhere to the laws of the United States and regulations of the Department of Agriculture.

Induction of experimental colitis by TNBS

To induced TNBS-colitis, epicutaneous skin sensitization with the hapten, tri-nitro-benzosulfonic acid (TNBS) (1% v/v; EtOH; Sigma Chemical) was performed under anesthesia on experimental day -7 in 8-10 weeks old mice (*C57BL/6J/6J, Lck Cre*$^+$, *Hif-2α*$^{loxP/loxP}$ *Lck Cre*$^+$, *miR-29a*$^{loxP/loxP}$ *Lck Cre*$^+$, *Cre*$^-$ littermates or *LSL-HIF2dPA Lck Cre*$^+$). On experimental day 0, anesthetized mice received challenge of intrarectal TNBS (5ul/g; 2.5% v/v; 40% EtOH), using a 20-gauge soft tygon plastic catheter. Vehicle control animals received a corresponding volume of 40% (v/v) ethanol alone. Body weight loss and disease activity indices (DAI's) were assessed daily. Control mice for each group included *Cre*$^-$ littermates or in separate experiments *Lck Cre*$^+$ control mice and no significant experimental differences between these two types of controls was noted.

Induction of chronic colitis by DSS

Mice were given Dextran Sodium Sulfate Salt (40,000 Sigma-Aldrich) in drinking water at 3% for 6 days, followed by two weeks of drinking water. 6-day DSS course was then repeated to induce chronic colitis. Body weight, occult and disease activity were assessed daily.

Induction of experimental colitis by adoptive transfer

B6.RAG1-/- (129S7(B6)-Rag1^{tm1Mom}*/J* were obtained from the Jackson laboratory and maintained by inhouse breeding in autoclaved housing. 6-8 weeks old male mice were transferred to standard housing and used as recipients of adoptive T cell transfer. Naïve $CD4^+$ T cells were purified with magnetic beads, labeled with fluorescent antibodies against CD4 and CD45RB (both from

Body weight and disease scores were recorded three times per week.

Human subjects

All human studies were approved by the institutional review board of the University of Colorado Denver. CD and UC patients were diagnosed using established criteria and CD phenotype per the Montreal criteria[80] (see Supplementary Table 1 for patient characteristics). Patient medications and demographics were recorded at the time of endoscopic evaluation, during which intestinal mucosal biopsies were obtained. Disease activity was determined based upon endoscopic evidence of mucosal inflammation. Informed, written consent was obtained from all patients prior to inclusion in the study. All data was de-identified before sample analysis and only patient age, disease duration and current IBD medication usage were reported to the researchers performing the sample analysis.

Luciferase imaging of T cell-intrinsic HIF activity in vivo

At time of euthanasia, mice were injected intraperitoneally with 300 mg/kg body weight D-luciferin (Calliper or Invitrogen, cat# L2916). Colons and small intestines were used for bioluminescence imaging using the IVIS Imaging System 50 Series (Calliper Life Sciences/Xenogen Corp.). Quantification was performed using Living Image v4.7.2 software. After imaging, mouse tissues were fixed with 4% paraformaldehyde (PFA) solution and paraffin-embedded for analysis of morphology and immunohistochemistry.

Measurement of cellular hypoxia by EF5-flow cytometry

Localization and quantitation of 2-nitroimidazole EF5 binding in hypoxic tissue was used to allow the assessment of hypoxia in the infiltrating T cells during colitis. Colitic mice described in Fig. 1a, b received a 200ul intraperitoneal injection of EF5 (Millipore Sigma) at 30 mg/kg 3 h prior to euthanasia and tissue harvest. EF5 binding was assessed in isolated $CD4^+$ T cell subsets with or without experimental colitis via flow cytometry with an anti-EF5-Cy5 conjugate (5.625ug; clone ELK3-51, Millipore EF5012). A matched isotype antibody (IgG1 CY5, Clone: 15H6, Southern Biotech) was utilized as a negative staining control. Cells were stained and gated on: singlets, live, $MHCII^-$, $CD3^+$, $CD4^+$ and effector memory T cells were additionally gated on $CD44^+$ and $CD62L^-$. Antibodies used were as follows: anti-CD4-FITC (Clone: GK1.5, Cat#: 11-0041-82, Invitrogen), 1:400, anti-CD45RB-PE (Clone: C363.16A, Cat#: 12-0455-82, Invitrogen), 1:600, anti-CD4-eFluor450 (Clone: GK1.5, Cat#: 48-0041-82, Invitrogen), 1:400, anti-CD8a-PE (Clone: 53-6.7, Cat#: 100707, BioLegend), 1:400, anti-CD8a-Pacific Blue (Clone: 53-6.7, Cat#: 100728, BioLegend), 1:400, anti-CD62L-APC (Clone: MEL-14, Cat#: 17-0621-82, Invitrogen), 1:500, anti-CD44-FITC (Clone: IM7, Cat#: 11-0441-82, Invitrogen), 1:200.

Cell isolation

Splenocytes, MLN, and colonic lamina propria mononuclear cells were isolated following experimental colitis experiments as previously described[81]. Intestinal epithelial cells and colonic lamina propria mononuclear cells in Figs. 2, 5e, 5f and Fig. 6 were prepared using Lamina Propria Dissociation Kit from Miltenyi Biotec (Cat# 130 097 410) per the manufacturer's protocol and subjected to Percoll gradient (Percoll P4937, Sigma-Aldrich) prior to restimulation and flow cytometry analysis.

Histology

Colons were excised, opened longitudinally and washed with cold PBS followed subsequently by 10% buffered formalin fixation. Tissue was then paraffin-embedded, cut into 5μm sections and stained with hematoxylin/eosin. Histological assessment of colitis sores was performed in a blinded fashion, as previously described[8].

Primary T cell isolation

T cells were purified from the spleens and peripheral lymph nodes of mice, mechanically disrupted into a single cell suspension, and subjected to magnetic bead enrichment for $CD4^+$ T cells, using either the $CD4^+$ T cell isolation kit (130-104-453, Miltenyi Biotec), Dynabeads™

Untouched™ Mouse CD4 Cells Kit (11415D, Invitrogen) or EasySep™ Mouse CD4 +T Cell Isolation Kit (19852, StemCell).

Enriched $CD4^+$ T cells were then subjected to FACS purification on a FACS Aria II (BD), with naïve $CD4^+$ T cells purified on the basis of the cell surface phenotype $CD4^+$ $CD45Rb^{high}CD62L^{high}CD25^{neg}CD44^{neg}$ in Fig. 1a, b, or with naïve T cells selected by $CD4^{pos}CD45RB^{high}CD25^{neg}$ or $CD4^{pos}CD45RB^{low}$(control) on a FACS Aria II (BD) in all subsequent adoptive transfer experiments. Antibodies used were as follows: anti-CD62L-APC (Clone: MEL-14, Cat#: 17-0621-82, Invitrogen), 1:500, anti-CD44-FITC (Clone: IM7, Cat#: 11-0441-82, Invitrogen), 1:200, anti-CD25-PB (Clone PC61.5 Cat#: 404-0251-82, Invitrogen), 1:400, anti-CD4-FITC (Clone: GK1.5, Cat#: 11-0041-82, Invitrogen), 1:400, anti-CD45RB-PE (Clone: C363.16A, Cat#: 12-0455-82, Invitrogen), 1:600, anti-CD62L-APC (Clone: MEL-14, Cat#: 17-0621-82, Invitrogen), 1:500.

In vitro T cell culture

Purified primary mouse and human $CD4^+$ T cells were cultured (1×10^6) cells/ml in RPMI-1640 (Gibco) containing FBS (5% v/v), L-glutamine (1% v/v), Antibiotic Antimycotic Solution at 1X (A5955, Sigma Aldrich), and β-mercaptoethanol (50 μM). $CD4^+$ T cells were stimulated with plate-bound anti-CD3ε (1 μg; clone 145-2C11; Cat#: 100359, BioLegend), soluble anti-CD28 (2 μg/ml; Clone: 37.51, Cat#: 102121, BioLegend) and supplemented with 10 ng/mL of recombinant mouse IL-2 (eBioscience). For differentiation of $CD4^+$ helper lineages, naïve $CD4^+$ $CD25^{neg}CD62L^+$ T cells were harvested from spleen of 6–10 weeks old mice by magnetic bead enrichment and cultured ex vivo for 3-5 days in lineage-polarizing conditions. Briefly, T_H0 T cells were maintained with the addition of recombinant IL-2 (200 U/ml; Peprotech), anti-IL-12 (C17.8, Catalog #BE0051, BioXCell) 10 μg/ml, anti-IFNγ (Clone XMG1.2, Catalog #BE0055, BioXCell) 10 μg/ml and anti-IL-4 (11B11, Catalog #BE0045, 10 μg/ml; BioXCell). T_H1 differentiation was achieved with the addition of recombinant IL-2 (10 ng/ml; Peprotech) and anti-IL-4 (10 μg/ml; BioXCell). T_H2 were differentiated with the addition of recombinant IL-4 (10 ng/ml; RnD systems) and anti-IFNγ (10 μg/ml; BioXCell). T_H17 were differentiated with recombinant TGFβ (5 ng/ml; RnD systems), IL-23 (10 ng/ml, RnD systems), IL-6 (20 ng/ml; RnD systems), anti-IL-4 (10 μg/ml; BioXCell) and anti-IFNγ (10 μg/ml; BioXCell). Lastly, T_{reg} cells were differentiated with the addition of recombinant TGFβ (15 ng/ml, RnD systems), IL-2 (200 U/ml, Peprotech), anti-IL-12, anti-IFNγ and anti-IL-4 (10 μg/ml; BioXCell). In a subset of experiment, pharmacologic stabilization of HIF with the PHD inhibitor, Dimethyloxallyl Glycine (DMOG; Calbiochem) was used under conditions of normoxia (21% O_2) or hypoxia (1% O_2). In Fig. 6 and Supplementary Fig. 4 and 5, T cells were differentiated exactly as above but the antibodies used for differentiation conditions were as follows: anti-IFNγ (Clone: XMG1.2, Cat#: 505847, BioLegend), 10ug/ml anti-IL-4 (Clone: 11B11, Cat#: 504136, BioLegend), 5ug/ml, anti-IL-2 (Clone: JES6-1A12, Cat#: 503707, BioLegend), 5ug/ml.

T cell culture and transfection with miRNAs

T_H1 skewed (day 3) CD4+ T cells were rested overnight in fresh medium. Subsequently, the T cells were transfected with 100 nM miRNA mimetic or 300 nM miRNA inhibitor (both from Dharmacon, Lafayette, CO) using Lipofectamine 3000 (Invitrogen), following the manufacturer's recommendations. Twelve hours after transfection cells were re-stimulated with 5.0 μg/ml anti-CD3/anti-CD28 mAbs (Cat#: 100359, 102121, BioLegend) and collected for further analysis 48 h later.

microRNA and mRNA transcriptional analysis

Total RNA or separated fractions of miRNA and mRNA were isolated from in vitro differentiated T cells or whole colon tissues using QIAzol Reagent (Cat. # 79306) and RNeasy kit (Cat.# 74104) following manufacturer instructions (Qiagen). Transcript levels were determined by real-time RT-PCR using specific primer sets (Qiagen and ThermoFisher) with Bio-Rad CFX384 system. Expression levels of miRNA's were normalized to endogenous RNU-6, while 18 s was used to normalize mRNA expression profiles. Limited target q-PCR based array with miRNA-specific primers from Qiagen (custom array) and Bio-Rad CFX384 system was used to measure changes in T cell-specific microRNAs shown in Fig. 2a; data was then normalized to the expression of RNU6 and further compared to the average of normoxia samples to create the heatmap. RNA for the array was prepared from T cells stimulated with anti-CD3/anti-CD28 mAbs (Cat#: 100359, 102121, BioLegend) for 8 h in normoxia and hypoxia.

Flow cytometry

Cells from indicated in vivo compartments or cell culture experiments, or cells prepared for FACS sorting were incubated with fluorescently labeled anti-mouse antibodies against: anti-CD4-FITC (Clone: GK1.5, Cat#: 11-0041-82, Invitrogen), 1:400, anti-CD8a-PE (Clone: 53-6.7, Cat#: 100707, BioLegend), 1:400, anti-CD62L-APC (Clone: MEL-14, Cat#: 17-0621-82, Invitrogen), 1:500, anti-CD44-FITC (Clone: IM7, Cat#: 11-0441-82, Invitrogen), 1:200, anti-IFNγ-APC (Clone: XMG1.2, Cat#: MABF1515, Sigma-Aldrich), 1:400, anti-IL-17a-PE (Clone:TC11-18H10.1, Cat#: 506903, BioLegend), 1:400, anti-TNFα-PE (Clone: TN3-19.12, Cat#: 506104, BioLegend), 1:400, anti-T-bet-PE (Clone: O4-46, Cat#: 561268, BD Bioscience), 1:400, anti-T-bet-BV421 (Clone: O4-46, Cat#: 563318, BD Bioscience), 1:400, anti-CD45RB-PE (Clone: C363.16A, Cat#: 12-0455-82, Invitrogen), 1:600 (eBioscience), or corresponding isotype controls. Intracellular staining was performed using the FoxP3 staining kit (eBioscience) according to the manufacturer's instructions. Intracellular cytokine staining was performed following 4 h of stimulation with PMA, Ionomycin and Brefeldin A. Analysis was performed using a BD FACS Canto™ II (BD Biosciences) or CytoFLEX LX (Beckman Coulter Lifesciences). Cell sorting was performed using a BD FACS Aria II (BD Biosciences). Further data analyses were performed using FLOWJo software (Tree Star Inc, Ashland, OR). Example of gating strategy used for T cells is provided in Supplementary Fig. 7.

Chromatin immuno-precipitation (ChIP) assay

ChIP was performed to assess DNA-protein interactions at the promoter sequences using the ChIP assay kit (Cell Signaling Technologies #9004) according to the manufacturer's instructions. Briefly, CD4 T cells were purified with magnetic beads and activated with anti-CD3/anti-CD28 mAbs (Cat#: 100359, 102121, BioLegend) under hypoxia for 8 h and subsequently harvested. Protein-DNA complexes were cross-linked by fixing with 1% (v/v) formaldehyde in a culture medium for 10 min. Cross-linking was stopped by 5 min of incubation with 125 mM glycine and nuclear contents were subsequently extracted. Chromatin was digested with Micrococcal Nuclease (MNase, provided from the kit) to yield fragments between 150–300 bp and the DNA was then immunoprecipitated overnight at 4 °C with 2 μg antibody specific to HIF2A (NB100-122, Novus) or control isotype Rabbit IgG (#2729, Cell Signaling Technologies). The DNA-antibody complexes were pull-down with agarose beads. The complexes were eluted from the beads and cross-linking was reversed by incubation for 2.5 h at 65 °C with proteinase K. Reaction was then stopped, and DNA products were analyzed by real-time PCR using the following primer pairs: HRE1- For GCGATCCTATGCTGACCTCA, HRE1- Rev CTGTCCCACGTCTGCTCTC, HRE2-For GAGCTCAGCACACTTTTGATAAG, HRE2-Rev TGTGTTGCTTTGCCTTTGAGA, HRE3-For CCCTTTATCCCTTCCTGCTCAT, HRE3-Rev ATGGACTAAGCCGGCTGTAG. Only 3 proximal HREs were assayed and the remaining 4 distant putative HREs were not assessed for binding.

In vivo nanoparticle delivery of mmu-miR-29a mimetic

To utilize a pharmacological approach to overexpress mmu-miR-29a during experimental TNBS-colitis, a nanoliposomal-based approach was employed to transport synthetic mmu-miR-29a. DOPC consists of 1,2-dioleoyl-sn-glycero-3-phosphocholine, squalene oil, polysorbate 20, and an antioxidant which when in complex with synthetic miRNAs

can form nanoparticles in the nanometer diameter[82] range. Packaging of the microRNA mimics was performed as described previously[83]. Mice were treated on indicated days during the course of colitis or ileitis with 50 μg synthetic mmu-miR-29a mimic (Dharmacon, Lafayette, CO) or respective control (mimic-ctr) formulated with LNP by intravenous retro-orbital injection.

Statistical analysis

Mice were randomized into experimental groups, and both male and female mice were used in all studies with the exception of transfer colitis where only male mice were used as recipients of the adoptive transfers. All experimental, disease and histological scoring was performed by researchers blinded to the identity of the samples.

Statistical analyses were performed using GraphPad Prism 8 software, and *t* test and one-way ANOVA or two-way ANOVA tests were used as indicated, respectively. Data were expressed as mean ± standard error of the mean (S.E.M). Statistical significance was set at $p < 0.05$.

Diagrams in Fig. 7 were prepared with BioRender.com

Reporting summary

Further information on research design is available in the Nature Portfolio Reporting Summary linked to this article.

Data availability

Source Data file containing all data points is provided with this manuscript. Data set that includes reads from the limited T-cell focused microRNA PCR-based microarray from Qiagen (first generation) is provided as Supplementary Data 1 (titled T-cell microarray). Any additional requests for information can be directed to, and will be fulfilled by, the corresponding authors. Source data are provided with this paper.

References

1. Karhausen, J. et al. Epithelial hypoxia-inducible factor-1 is protective in murine experimental colitis. *J. Clin. Invest.* **114**, 1098–1106 (2004).
2. Colgan, S. P. & Taylor, C. T. Hypoxia: an alarm signal during intestinal inflammation. *Nat. Rev. Gastroenterol. Hepatol.* **7**, 281–287 (2010).
3. Clambey, E. T. et al. Hypoxia-inducible factor-1 alpha-dependent induction of FoxP3 drives regulatory T-cell abundance and function during inflammatory hypoxia of the mucosa. *Proc. Natl Acad. Sci. USA* **109**, E2784–E2793 (2012).
4. Kominsky, D. J. et al. An endogenously anti-inflammatory role for methylation in mucosal inflammation identified through metabolite profiling. *J. Immunol.* **186**, 6505–6514 (2011).
5. Glover, L. E. et al. Control of creatine metabolism by HIF is an endogenous mechanism of barrier regulation in colitis. *Proc. Natl Acad. Sci. USA* **110**, 19820–19825 (2013).
6. Giatromanolaki, A. et al. Hypoxia inducible factor 1alpha and 2alpha overexpression in inflammatory bowel disease. *J. Clin. Pathol.* **56**, 209–213 (2003).
7. Harris, N. R. et al. Relationship between inflammation and tissue hypoxia in a mouse model of chronic colitis. *Inflamm. Bowel Dis.* **17**, 742–746 (2011).
8. Campbell, E. L. et al. Transmigrating neutrophils shape the mucosal microenvironment through localized oxygen depletion to influence resolution of inflammation. *Immunity* **40**, 66–77 (2014).
9. Bowser, J. L., Phan, L. H. & Eltzschig, H. K. The hypoxia-adenosine link during Intestinal Inflammation. *J. Immunol.* **200**, 897–907 (2018).
10. Brown, E. & Taylor, C. T. Hypoxia-sensitive pathways in intestinal inflammation. *J. Physiol.* **596**, 2985–2989 (2018).
11. Steiner, C. A., Cartwright, I. M., Taylor, C. T. & Colgan, S. P. Hypoxia-inducible factor as a bridge between healthy barrier function, wound healing, and fibrosis. *Am. J. Physiol. Cell Physiol.* **323**, C866–c878 (2022).
12. Sartor, R. B. Cytokines in intestinal inflammation: pathophysiological and clinical considerations. *Gastroenterology* **106**, 533–539 (1994).
13. Breese, E., Braegger, C. P., Corrigan, C. J., Walker-Smith, J. A. & MacDonald, T. T. Interleukin-2- and interferon-gamma-secreting T cells in normal and diseased human intestinal mucosa. *Immunology* **78**, 127–131 (1993).
14. Fuss, I. J. et al. Disparate CD4+ lamina propria (LP) lymphokine secretion profiles in inflammatory bowel disease. Crohn's disease LP cells manifest increased secretion of IFN-gamma, whereas ulcerative colitis LP cells manifest increased secretion of IL-5. *J. Immunol.* **157**, 1261–1270 (1996).
15. Neurath, M. F. et al. The transcription factor T-bet regulates mucosal T cell activation in experimental colitis and Crohn's disease. *J. Exp. Med.* **195**, 1129–1143 (2002).
16. Krausgruber, T. et al. T-bet is a key modulator of IL-23-driven pathogenic CD4(+) T cell responses in the intestine. *Nat. Commun.* **7**, 11627 (2016).
17. Dang, E. V. et al. Control of T(H)17/T(reg) balance by hypoxia-inducible factor 1. *Cell* **146**, 772–784 (2011).
18. Hsu, T. S. et al. HIF-2α is indispensable for regulatory T cell function. *Nat. Commun.* **11**, 5005 (2020).
19. Imam, T., Park, S., Kaplan, M. H. & Olson, M. R. Effector T helper cell subsets in inflammatory bowel diseases. *Front. Immunol.* **9**, 1212–1212 (2018).
20. Singh, Y., Garden, O. A., Lang, F. & Cobb, B. S. MicroRNAs regulate T-cell production of interleukin-9 and identify hypoxia-inducible factor-2α as an important regulator of T helper 9 and regulatory T-cell differentiation. *Immunology* **149**, 74–86 (2016).
21. Manalo, D. J. et al. Transcriptional regulation of vascular endothelial cell responses to hypoxia by HIF-1. *Blood* **105**, 659–669 (2005).
22. Ju, C. et al. Hypoxia-inducible factor-1alpha-dependent induction of miR122 enhances hepatic ischemia tolerance. *J. Clin. Invest.* **131**, e140300 (2021).
23. Lee, T. J. et al. Strategies to modulate MicroRNA functions for the treatment of cancer or organ injury. *Pharm. Rev.* **72**, 639–667 (2020).
24. Bartel, D. P. MicroRNAs: target recognition and regulatory functions. *Cell* **136**, 215–233 (2009).
25. Han, Y. C. et al. microRNA-29a induces aberrant self-renewal capacity in hematopoietic progenitors, biased myeloid development, and acute myeloid leukemia. *J. Exp. Med.* **207**, 475–489 (2010).
26. Ju, C. et al. Hypoxia-inducible factor-1α-dependent induction of miR122 enhances hepatic ischemia tolerance. *J. Clin. Invest.* **131**, e140300 (2021).
27. Stelekati, E. et al. MicroRNA-29a attenuates CD8 T cell exhaustion and induces memory-like CD8 T cells during chronic infection. *Proc. Natl Acad. Sci.* **119**, e2106083119 (2022).
28. Muljo, S. A. et al. Aberrant T cell differentiation in the absence of Dicer. *J. Exp. Med.* **202**, 261–269 (2005).
29. O'Connell, R. M., Rao, D. S., Chaudhuri, A. A. & Baltimore, D. Physiological and pathological roles for microRNAs in the immune system. *Nat. Rev. Immunol.* **10**, 111–122 (2010).
30. Cho, S., Dong, J. & Lu, L. F. Cell-intrinsic and -extrinsic roles of miRNAs in regulating T cell immunity. *Immunol. Rev.* **304**, 126–140 (2021).
31. Steiner, D. F. et al. MicroRNA-29 regulates T-box transcription factors and interferon-gamma production in helper T cells. *Immunity* **35**, 169–181 (2011).
32. Ma, F. et al. The microRNA miR-29 controls innate and adaptive immune responses to intracellular bacterial infection by targeting interferon-γ. *Nat. Immunol.* **12**, 861–869 (2011).
33. Smith, K. M. et al. miR-29ab1 deficiency identifies a negative feedback loop controlling Th1 bias that is dysregulated in multiple sclerosis. *J. Immunol.* **189**, 1567–1576 (2012).

34. Colgan, S. P., Furuta, G. T. & Taylor, C. T. Hypoxia and Innate Immunity: Keeping Up with the HIFsters. *Annu. Rev. Immunol.* **38**, 341–363 (2020).
35. McNamee, E. N., Korns Johnson, D., Homann, D. & Clambey, E. T. Hypoxia and hypoxia-inducible factors as regulators of T cell development, differentiation, and function. *Immunol. Res.* **55**, 58–70 (2013).
36. Safran, M. et al. Mouse model for noninvasive imaging of HIF prolyl hydroxylase activity: assessment of an oral agent that stimulates erythropoietin production. *Proc. Natl Acad. Sci. USA* **103**, 105–110 (2006).
37. Kriegel, A. J., Liu, Y., Fang, Y., Ding, X. & Liang, M. The miR-29 family: genomics, cell biology, and relevance to renal and cardiovascular injury. *Physiol. Genomics* **44**, 237–244 (2012).
38. Hu, C. J., Wang, L. Y., Chodosh, L. A., Keith, B. & Simon, M. C. Differential roles of hypoxia-inducible factor 1alpha (HIF-1alpha) and HIF-2alpha in hypoxic gene regulation. *Mol. Cell. Biol.* **23**, 9361–9374 (2003).
39. Thiel, M. et al. Targeted deletion of HIF-1alpha gene in T cells prevents their inhibition in hypoxic inflamed tissues and improves septic mice survival. *PLoS ONE* **2**, e853 (2007).
40. Zhang, J. et al. Hypoxia-Inducible Factor-2α Limits Natural Killer T Cell Cytotoxicity in Renal Ischemia/Reperfusion Injury. *J. Am. Soc. Nephrol.* **27**, 92–106 (2016).
41. Kim, W. Y. et al. Failure to prolyl hydroxylate hypoxia-inducible factor alpha phenocopies VHL inactivation in vivo. *EMBO J.* **25**, 4650–4662 (2006).
42. Eltzschig, H. K., Bratton, D. L. & Colgan, S. P. Targeting hypoxia signalling for the treatment of ischaemic and inflammatory diseases. *Nat. Rev. Drug Discov.* **13**, 852–869 (2014).
43. Hwang, H. W., Wentzel, E. A. & Mendell, J. T. A hexanucleotide element directs microRNA nuclear import. *Science* **315**, 97–100 (2007).
44. Wenger, R. H., Stiehl, D. P. & Camenisch, G. Integration of oxygen signaling at the consensus HRE. *Science's STKE: Signal Transduct. Knowl. Environ.* **2005**, re12 (2005).
45. Ma, F. et al. The microRNA miR-29 controls innate and adaptive immune responses to intracellular bacterial infection by targeting interferon-gamma. *Nat. Immunol.* **12**, 861–869 (2011).
46. Asseman, C., Fowler, S. & Powrie, F. Control of experimental inflammatory bowel disease by regulatory T cells. *Am. J. Respiratory Crit. Care Med.* **162**, S185–S189 (2000).
47. Powrie, F., Correa-Oliveira, R., Mauze, S. & Coffman, R. L. Regulatory interactions between CD45RBhigh and CD45RBlow CD4+ T cells are important for the balance between protective and pathogenic cell-mediated immunity. *J. Exp. Med.* **179**, 589–600 (1994).
48. Liu, H. P. et al. TGF-β converts Th1 cells into Th17 cells through stimulation of Runx1 expression. *Eur. J. Immunol.* **45**, 1010–1018 (2015).
49. Leppkes, M. et al. RORgamma-expressing Th17 cells induce murine chronic intestinal inflammation via redundant effects of IL-17A and IL-17F. *Gastroenterology* **136**, 257–267 (2009).
50. Yang, J. Patisiran for the treatment of hereditary transthyretin-mediated amyloidosis. *Expert Rev. Clin. Pharmacol.* **12**, 95–99 (2019).
51. Chen, X. et al. RNA interference-based therapy and its delivery systems. *Cancer Metastasis Rev.* **37**, 107–124 (2018).
52. Sanctuary, M. R. et al. miR-106a deficiency attenuates inflammation in murine IBD models. *Mucosal Immunol.* **12**, 200–211 (2019).
53. Cho, S. H. et al. Hypoxia-inducible factors in CD4(+) T cells promote metabolism, switch cytokine secretion, and T cell help in humoral immunity. *Proc. Natl Acad. Sci. USA* **116**, 8975–8984 (2019).
54. Higashiyama, M. et al. HIF-1 in T cells ameliorated dextran sodium sulfate-induced murine colitis. *J. Leukoc. Biol.* **91**, 901–909 (2012).
55. Phan, A. T. & Goldrath, A. W. Hypoxia-inducible factors regulate T cell metabolism and function. *Mol. Immunol.* **68**, 527–535 (2015).
56. Longhi, M. S., Moss, A., Jiang, Z. G. & Robson, S. C. Purinergic signaling during intestinal inflammation. *J. Mol. Med.* **95**, 915–925 (2017).
57. Fasseu, M. et al. Identification of restricted subsets of mature microRNA abnormally expressed in inactive colonic mucosa of patients with inflammatory bowel disease. *PLoS ONE* **5**, e13160 (2010).
58. Fredman, G., Li, Y., Dalli, J., Chiang, N. & Serhan, C. N. Self-limited versus delayed resolution of acute inflammation: temporal regulation of pro-resolving mediators and microRNA. *Sci. Rep.* **2**, 639 (2012).
59. Li, Y. et al. Plasticity of leukocytic exudates in resolving acute inflammation is regulated by MicroRNA and proresolving mediators. *Immunity* **39**, 885–898 (2013).
60. Ma, X., Zhang, H., Xue, X. & Shah, Y. M. Hypoxia-inducible factor 2α (HIF-2α) promotes colon cancer growth by potentiating Yes-associated protein 1 (YAP1) activity. *J. Biol. Chem.* **292**, 17046–17056 (2017).
61. Xue, X. et al. Hypoxia-inducible factor-2α activation promotes colorectal cancer progression by dysregulating iron homeostasis. *Cancer Res.* **72**, 2285–2293 (2012).
62. McGettrick, A. F. & O'Neill, L. A. J. The role of HIF in immunity and inflammation. *Cell Metab.* **32**, 524–536 (2020).
63. Shehade, H., Acolty, V., Moser, M. & Oldenhove, G. Cutting edge: hypoxia-inducible factor 1 negatively regulates Th1 function. *J. Immunol.* **195**, 1372–1376 (2015).
64. Bartel, D. P. Metazoan MicroRNAs. *Cell* **173**, 20–51 (2018).
65. Monticelli, S. et al. MicroRNA profiling of the murine hematopoietic system. *Genome Biol.* **6**, R71 (2005).
66. Wu, H. et al. miRNA profiling of naive, effector and memory CD8 T cells. *PLoS ONE* **2**, e1020 (2007).
67. Chong, M. M., Rasmussen, J. P., Rudensky, A. Y. & Littman, D. R. The RNAseIII enzyme Drosha is critical in T cells for preventing lethal inflammatory disease. *J. Exp. Med.* **205**, 2005–2017 (2008).
68. Eulalio, A., Schulte, L. & Vogel, J. The mammalian microRNA response to bacterial infections. *RNA Biol.* **9**, 742–750 (2012).
69. Hu, W. et al. miR-29a maintains mouse hematopoietic stem cell self-renewal by regulating Dnmt3a. *Blood* **125**, 2206–2216 (2015).
70. Papadopoulou, A. S. et al. The thymic epithelial microRNA network elevates the threshold for infection-associated thymic involution via miR-29a mediated suppression of the IFN-α receptor. *Nat. Immunol.* **13**, 181–187 (2011).
71. Horita, M., Farquharson, C. & Stephen, L. A. The role of miR-29 family in disease. *J. Cell. Biochem.* **122**, 696–715 (2021).
72. Chandiran, K. et al. Notch1 primes CD4 T cells for T helper type I differentiation through its early effects on miR-29. *Mol. Immunol.* **99**, 191–198 (2018).
73. van Nieuwenhuijze, A. et al. Defective germinal center B-cell response and reduced arthritic pathology in microRNA-29a-deficient mice. *Cell. Mol. Life Sci.* **74**, 2095–2106 (2017).
74. Cosin-Roger, J. et al. Hypoxia ameliorates intestinal inflammation through NLRP3/mTOR downregulation and autophagy activation. *Nat. Commun.* **8**, 98 (2017).
75. Keely, S. et al. Contribution of epithelial innate immunity to systemic protection afforded by prolyl hydroxylase inhibition in murine colitis. *Mucosal Immunol.* **7**, 114–123 (2014).
76. Marks, E. et al. Oral delivery of prolyl hydroxylase inhibitor: AKB-4924 promotes localized mucosal healing in a mouse model of colitis. *Inflamm. Bowel Dis.* **21**, 267–275 (2015).
77. Robinson, A. et al. Mucosal protection by hypoxia-inducible factor prolyl hydroxylase inhibition. *Gastroenterology* **134**, 145–155 (2008).
78. Sun, M. et al. Hypoxia inducible factor-1α-induced interleukin-33 expression in intestinal epithelia contributes to mucosal homeostasis in inflammatory bowel disease. *Clin. Exp. Immunol.* **187**, 428–440 (2017).

79. Fukata, T. et al. The supercarbonate apatite-MicroRNA complex inhibits dextran sodium sulfate-induced colitis. *Mol. Ther. Nucleic Acids* **12**, 658–671 (2018).
80. Satsangi, J., Silverberg, M. S., Vermeire, S. & Colombel, J. F. The Montreal classification of inflammatory bowel disease: controversies, consensus, and implications. *Gut* **55**, 749–753 (2006).
81. McNamee, E. N. et al. Novel model of TH2-polarized chronic ileitis: the SAMP1 mouse. *Inflamm. Bowel Dis.* **16**, 743–752 (2010).
82. Landen, C. N. Jr. et al. Therapeutic EphA2 gene targeting in vivo using neutral liposomal small interfering RNA delivery. *Cancer Res.* **65**, 6910–6918 (2005).
83. Elsayed, A. M. et al. PRKAR1B-AS2 long noncoding RNA promotes tumorigenesis, survival, and chemoresistance via the PI3K/AKT/mTOR pathway. *Int. J. Mol. Sci.* **22**, 1882 (2021).

Acknowledgements

The authors would like to thank the members of the Eltzschig lab, Kelley Brodsky and Eric T. Clambey for technical assistance with experimentation. We thank Frank Xuebo Chen for expert technical assistance with animal husbandry and breeding. Martine McManus performed the TNBS colitis scoring in Figs. 4, 5j and 7c. This work was supported by The Assistant Secretary of Defense for Health Affairs endorsed by the Department of Defense, in the amount of ($312,000), through the Peer Reviewed Medical Research Program under Award Number (HT9425-23-1-0094) to A.K.C. Opinions, interpretations, conclusions, and recommendations are those of the authors and are not necessarily endorsed by The Assistant Secretary of Defense for Health Affairs endorsed by the Department of Defense. The work was also supported by the National Institute of Health Grants R01-HL154720, R01-DK122796, R01-HL133900 and by a grant from the Crohn's and Colitis Foundation of America (CCFA) to H.K.E.; Crohn's and Colitis Foundation of America grants (CCFA #273007, #409992) and National Institute of Diabetes and Digestive and Kidney Diseases (# R01DK111856) to E.McN and E.DeZ. W.R. is supported by International Anesthesia Research Society (IARS) Mentored Research Award. X.Y. is supported by National Institute of Health Grants R01HL155950, Parker B. Francis Fellowship, and American Lung Association Catalyst Award CA-622265.

Author contributions

Conceptualization, H.K.E., A.K.C., and E.McN; Methodology; A.K.C., E.McN., E.T.C, J.C.M., C.B.C., H.K.E.; Investigation, A.K.C., E.McN., E.DeZ, X.H., V.V, T.C., I.B, J.C.M., E.T., C.B.C., S.F., H.L., T.N; Writing–Original Draft, A.K.C, E.McN., and H.K.E.; Writing–Review & Editing, A.K.C., E.McN, Y.W, X.H., W.R, E.DeZ, H.K.E.; Resources, A.S., M.McM., M.E.G., G.T.F, S.P.C., X.Y, C.R-A., G.L-B., H.K.E.; Supervision & Project administration, A.K.C., E.McN., and H.K.E.

Competing interests

The authors declare no competing interests.

Additional information

Supplementary information The online version contains supplementary material available at https://doi.org/10.1038/s41467-024-52113-y.

Correspondence and requests for materials should be addressed to Agnieszka K. Czopik or Edwin F. de Zoeten.

Peer review information *Nature Communications* thanks Maria Serena Longhi and the other, anonymous, reviewer(s) for their contribution to the peer review of this work. A peer review file is available.

Reprints and permissions information is available at http://www.nature.com/reprints

Publisher's note Springer Nature remains neutral with regard to jurisdictional claims in published maps and institutional affiliations.

[1]Department of Anesthesiology, Critical Care and Pain Medicine, McGovern Medical School, The University of Texas Health Science Center at Houston, Houston, TX, USA. [2]Mucosal Inflammation Program, University of Colorado Anschutz School of Medicine, Aurora, CO, USA. [3]Digestive Health Institute, Children's Hospital Colorado, Aurora, CO, USA. [4]Gastrointestinal Eosinophilic Disease Program University of Colorado Anschutz School of Medicine, Aurora, CO, USA. [5]Department of Pediatrics, University of Colorado Anschutz School of Medicine, Aurora, CO, USA. [6]Department of Convergence Medicine, Asan Medical Institute of Convergence Science and Technology (AMIST), Asan Medical Center, University of Ulsan College of Medicine, Seoul, Korea. [7]Organ Protection Program, Department of Anesthesiology, University of Colorado - Anschutz Medical Campus, Aurora, CO, USA. [8]Department of Anaesthesiology, LMU University Hospital, LMU Munich, Munich, Germany. [9]Division of Pulmonary Sciences and Critical Care Medicine, School of Medicine, University of Colorado - Anschutz Medical Campus, Aurora, CO, USA. [10]Departmental of Experimental Therapeutics and Center for RNA Interference and Non-Coding RNA, The University of Texas MD Anderson Cancer Center, Houston, TX, USA. [11]Division of Gastroenterology & Hepatology, University of Colorado Anschutz School of Medicine, Aurora, CO, USA. [12]Department of Gynecologic Oncology and Reproductive Medicine, The University of Texas MD Anderson Cancer Center, Houston, TX, USA. [13]Center for Outcomes Research, Department of Anesthesiology, Critical Care and Pain Medicine, McGovern Medical School, The University of Texas Health Science Center, Houston, TX, USA. [14]These authors contributed equally: Agnieszka K. Czopik, Eóin N. McNamee.
✉e-mail: Agnieszka.K.Czopik@uth.tmc.edu; Edwin.DeZoeten@childrenscolorado.org